



1 **MIXv2: a long-term mosaic emission inventory for**
2 **Asia (2010-2017)**

3

4 **Meng Li^{1,2}, Junichi Kurokawa³, Qiang Zhang⁴, Jung-Hun Woo^{5,6}, Tazuko Morikawa⁷, Satoru**
5 **Chatani⁸, Zifeng Lu⁹, Yu Song¹⁰, Guannan Geng¹¹, Hanwen Hu¹¹, Jinseok Kim⁶, Owen R. Cooper^{1,2},**
6 **Brian C. McDonald²**

7 ¹ Cooperative Institute for Research in Environmental Sciences, University of Colorado, Boulder, CO,
8 USA

9 ² NOAA Chemical Sciences Laboratory, Boulder, CO, USA

10 ³ Asia Center for Air Pollution Research, 1182 Sowa, Nishi-ku, Niigata, Niigata, 950-2144, Japan

11 ⁴ Ministry of Education Key Laboratory for Earth System Modeling, Department of Earth System
12 Science, Tsinghua University, 100084 Beijing, China

13 ⁵ Department of Civil and Environmental Engineering, Konkuk University, Seoul, Republic of Korea

14 ⁶ Department of Technology Fusion Engineering, Konkuk University, Seoul, Republic of Korea

15 ⁷ Japan Automobile Research Institute, 2530 Karima, Tsukuba, Ibaraki, 305-0822, Japan

16 ⁸ National Institute for Environmental Studies, 16-2 Onogawa, Tsukuba, Ibaraki, 305-8506, Japan

17 ⁹ Energy Systems and Infrastructure Analysis Division, Argonne National Laboratory, Lemont, IL, USA

18 ¹⁰ State Key Joint Laboratory of Environmental Simulation and Pollution Control, Department of
19 Environmental Science, Peking University, Beijing, People's Republic of China

20 ¹¹ State Key Joint Laboratory of Environmental Simulation and Pollution Control, School of Environment,
21 Tsinghua University, Beijing, China

22

23

24

25

26

27

28 *Correspondence to:* Meng Li (Meng.Li-1@colorado.edu)

29

30



31 **Abstract**

32 The MIXv2 Asian emission inventory is developed under the framework of the Model Inter-
33 Comparison Study for Asia (MICS-Asia) Phase IV, and produced from a mosaic of up-to-date
34 regional emission inventories. We estimated the emissions for anthropogenic and biomass
35 burning sources covering 23 countries and regions in East, Southeast and South Asia, and
36 aggregated emissions to a uniform spatial and temporal resolution for seven sectors: power,
37 industry, residential, transportation, agriculture, open biomass burning and shipping. Compared
38 to MIXv1, we extended the dataset to 2010 – 2017, included emissions of open biomass burning
39 and shipping, and provided model-ready emissions of SAPRC99, SAPRC07, and CB05. A series
40 of unit-based point source information was incorporated covering power plants in China and
41 India. A consistent speciation framework for Non-Methane Volatile Organic Compounds
42 (NMVOCs) was applied to develop emissions by three chemical mechanisms. The total Asian
43 emissions for anthropogenic | open biomass sectors in 2017 are estimated as follows: 41.6 | 1.1
44 Tg NO_x, 33.2 | 0.1 Tg SO₂, 258.2 | 20.6 Tg CO, 61.8 | 8.2 Tg NMVOC, 28.3 | 0.3 Tg NH₃, 24.0 |
45 2.6 Tg PM₁₀, 16.7 | 2.0 Tg PM_{2.5}, 2.7 | 0.1 Tg BC, 5.3 | 0.9 Tg OC, and 18.0 | 0.4 Pg CO₂. The
46 contributions of India and Southeast Asia have been emerging in Asia during 2010-2017,
47 especially for SO₂, NH₃ and particulate matters. Gridded emissions at a spatial resolution of 0.1
48 degree with monthly variations are now publicly available at
49 <https://csl.noaa.gov/groups/csl4/modeldata/data/Li2023/>.

50

51

52 **1. Introduction**

53 The Model Inter-Comparison Study for Asia (MICS-Asia) is a research project currently in its
54 fourth phase, MICS-Asia IV, which aims to advance our understanding of the discrepancies and
55 relative uncertainties present in the simulations of air quality and climate models (Chen et al.,
56 2019; Gao et al., 2018; Itahashi et al., 2020; Li et al., 2017c). A critical component of the project
57 is ensuring that emission inventories remain consistent across various atmospheric and climate
58 models. In support of MICS-Asia IV research activities and related policy-making endeavors, we
59 developed MIXv2, the second version of our mosaic Asian inventory. MIXv2 combines the best
60 available state-of-the-art regional emission inventories from across Asia using a mosaic
61 approach. This inventory is expected to enhance our capabilities to assess emission changes and
62 their driving forces, and their impact on air quality and climate change, thus providing valuable
63 insights for decision-makers and stakeholders.

64 The first version of MIX Asian inventory (MIXv1) has been widely applied to support scientific
65 research activities from regional to local scales (Geng et al., 2021; Hammer et al., 2020; Li et al.,
66 2019a; Li et al., 2017c). MIXv1 incorporates five regional emission inventories for all major
67 anthropogenic sources over Asia, providing a gridded emission dataset at a spatial resolution of
68 0.25 degree for 2008 and 2010. The mosaic approach has been proved to increase the emission
69 accuracy and model performance significantly by including more local information (Li et al.,



70 2017c). A profile-based speciation scheme for Non-Methane Volatile Organic Compounds
71 (NMVOCs) was applied to develop model-ready emissions by chemical mechanisms, which
72 reduced the uncertainties arising from inaccurate mapping between inventory and model species
73 (Li et al., 2014; Li et al., 2019b). Specifically, MIXv1 advances our understanding of emissions
74 and spatial distributions from power plants and agricultural activities through a mosaic of unit-
75 based information and a process-based model.

76 Tremendous efforts have been made continuously to improve air quality and protect human
77 health in Asia since 2010, and these effects on emission abatement need to be updated in
78 inventories (Zheng et al., 2018). In this regard, a long-term inventory with updated information is
79 critical. However, it's difficult to develop consistent emissions over Asia for a long period using
80 the mosaic approach because of the lack of available regional inventory data. Within the MICS-
81 Asia community, developers of regional inventories have been endeavoring to extend their
82 emission inventories to the present day since Phase IV. Through intensive collaboration and
83 community efforts, we now have a complete list of available regional emission inventories
84 covering major parts of Asia, and are able to combine them to produce a new version of MIX for
85 2010-2017.

86 Consistent greenhouse gas emissions are crucial for climate-air quality nexus research and
87 policymaking (Fiore et al., 2015). Carbon dioxide (CO₂) is co-emitted with many air pollutants
88 which are contributors of ozone and particulate matter, further changing climate through forcings
89 of Earth's radiation budget (Fiore et al., 2015). Previous studies have emphasized the importance
90 of air pollution mitigation and climate change (Jacob and Winner, 2009; Saari et al., 2015), as
91 recently summarized by the Synthesis Report of the IPCC Sixth Assessment Report (IPCC:
92 Intergovernmental Panel on Climate Change, report available at
93 <https://www.ipcc.ch/report/sixth-assessment-report-cycle/>). Given the common sources of CO₂
94 and air pollutants, it's important to quantify their emissions distribution in a self-consistent way
95 to assess the co-benefits and pathways to cleaner air and carbon neutrality (Klausbruckner et al.,
96 2016; Phillips, 2022; von Schneidemesser and Monks, 2013). To address this need, CO₂
97 emissions are estimated based on the same emission inventory framework as the short-lived air
98 pollutants, and further integrated into MIXv2 following the mosaic methodology.

99 Compared to MIXv1, MIXv2 has the following updates:

- 100 - advances the horizontal resolution of the gridded maps from 0.25 to 0.1 degree
- 101 - incorporates up-to-date regional inventories from 2010-2017
- 102 - provides emissions of open biomass burning and shipping, in addition to anthropogenic sources
- 103 - develops model-ready emissions of SAPRC99, SAPRC07 and CB05

104 Methods and input data are described in Sect. 2. Emissions evolution and their driving forces,
105 seasonality, spatial distribution, NMVOC speciation and inventory limitations are analyzed and
106 discussed in Sect. 3. Sect. 4 compares the MIX data with other bottom-up and top-down
107 emission estimates. Concluding remarks are provided in Sect. 5.

108



109 **2. Methods and Inputs**

110 **2.1 Overview of MIXv2**

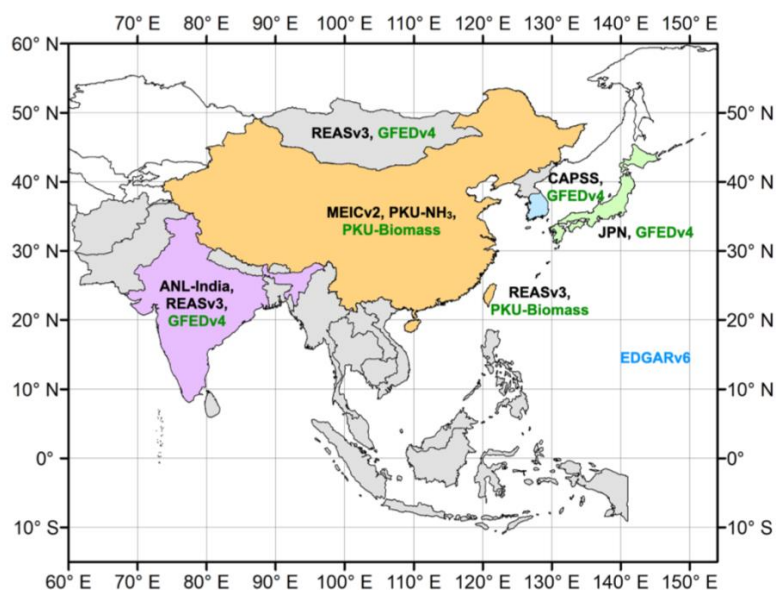
111 The key features of MIXv2 are summarized in Table 1. Anthropogenic sources, including power,
112 industry, residential, transportation and agriculture, along with open biomass burning and
113 shipping are included. Dust and aviation are not included in the current version of MIX. Monthly
114 emissions between 2010 – 2017 are allocated to grids at 0.1×0.1 degree. Emissions of ten
115 species, including CO₂ and air pollutants of NO_x, SO₂, CO, NMVOC, NH₃, PM₁₀, PM_{2.5}, BC and
116 OC are estimated. MIX can support most atmospheric models compatible with gas-phase
117 chemical mechanisms of SAPRC99, SAPRC07, CB05, and those can be mapped based on these
118 three chemical mechanisms (e.g., GEOS-Chem, MOZART) (Li et al., 2014). As shown in Figure
119 1, MIXv2 stretches from Afghanistan in the west to Japan in the east, from Indonesia in the south
120 to Mongolia in the north. The domain is consistent with the REASv3 gridded emissions product.

121 Table 2 summarizes the subsectors for each sector in the development of MIX, along with the
122 corresponding source codes used by IPCC.

123

124 **2.2 Mosaic Methodology**

125 We follow a mosaic methodology similar to the development of MIXv1 (Li et al., 2017c), as shown
126 in Figure 1. In brief, seven regional emission inventories were collected and integrated into a
127 uniform format, including: the Regional Emission inventory in Asia version 3 for Asia (referred
128 to as REASv3) (Kurokawa and Ohara, 2020); the Multi-resolution Emission Inventory for China
129 version 2.0 (MEICv2, <http://www.meicmodel.org>) (Li et al., 2017b; Zheng et al., 2021; Zheng et
130 al., 2018); a process-based NH₃ emission inventory developed by Peking University (referred to
131 as PKU-NH₃) (Kang et al., 2016); an official Japan emission inventory (referred to as JPN)
132 (Chatani et al., 2018; Shibata and Morikawa, 2021); an Indian emission inventory for power plants
133 from Argonne National Laboratory (referred to as ANL-India) (Lu and Streets, 2012; Lu et al.,
134 2011); an open biomass burning emission inventory from Peking University (PKU-Biomass) (Yin
135 et al., 2019); the official emissions from Clean Air Policy Support System (CAPSS) for the
136 Republic of Korea (Lee et al., 2011); the fourth version of Global Fire Emissions Database with
137 small fires (GFEDv4s) (van der Werf et al., 2017); and the Emissions Database for Global
138 Atmospheric Research (EDGAR) version 6 for the shipping emissions (Janssens-Maenhout et al.,
139 2019). Figure 1 shows the distribution of the components of regional inventories which are
140 mosaicked into the MIXv2.



141

142 **Figure 1. Components of regional emission inventories in the MIXv2 mosaic. Colors of text**
143 **represent the type of sources: black is anthropogenic, dark green represents open biomass**
144 **burning, and blue is the inland and international shipping.**

145

146 We follow a similar hierarchy in MIXv2 as the previous version in the mosaic process. We use
147 REASv3 as the default inventory for anthropogenic sources, and then further replace it with
148 official emission inventories at a finer scale. MEIC, PKU-NH₃ and ANL-India are demonstrated
149 as the best available inventories through inter-comparisons to represent local source distribution
150 with advanced methodology and reliable data sources (Li et al., 2017c). Thus, MEIC overrides
151 REAS for anthropogenic emissions over mainland China. PKU-NH₃, which was developed with
152 a process-based model was further applied to replace the NH₃ emissions in MEIC. In Japan, JPN
153 provides emissions for all air pollutants. The ratios of CO₂ to NO_x by sectors derived from REAS
154 are combined with JPN to develop CO₂ gridded emissions. We use ANL-India for SO₂, NO_x and
155 CO₂ for power plants in India directly. To maintain consistency in spatial distribution, we re-
156 located REAS power plant emissions for other species to grids based on spatial proxies derived
157 from ANL-India. Regarding Hong Kong of China, we use the updated REASv3 emissions.

158 The open biomass emissions of MIX are developed by combining GFEDv4s and PKU-Biomass
159 inventories. GFED emissions over Asia are processed to the objective domain. We re-gridded the
160 GFED emissions from 0.25 to 0.1 degree based on an area-weighted algorithm in a mass-
161 balanced way. Wildfires of various vegetation types and in-field agricultural waste burning are
162 aggregated into the “open biomass burning” sector. PKU-Biomass overrides the emissions of
163 GFED over China (including Hong Kong and Taiwan) on both monthly and daily basis.



164

165

Table 1. Key features of MIXv2 and the component emission inventories.

Items	MIXv2	REASv3.3	MEICv2.0	PKU-NH ₃	ANL-India	JPN	CAPSS	PKU-Biomass	GFEDv4s	EDGARv6
Anthropogenic										
Power	X	X	X	X	X	X	X	X	X	X
Industry	X	X	X	X	X	X	X	X	X	X
Residential	X	X	X	X	X	X	X	X	X	X
Transportation	X	X	X	X	X	X	X	X	X	X
Agriculture	X	X	X	X	X	X	X	X	X	X
Open biomass burning	X	X	X	X	X	X	X	X	X	X
Shipping	X	X	X	X	X	X	X	X	X	X
Temporal coverage	2010-2017	1950-2017	1990-2017	1980-2017	2010-2017	2000-2017	2000-2018	1980-2017	2010-2017	1970-2018
Temporal resolution	Monthly	Monthly	Monthly	Monthly	Monthly	Monthly	Annual	Daily	Daily	Monthly
Spatial coverage	Asia	Asia	Mainland China	Mainland China	India	Japan	Korea, Republic of	China	Global	Global
Spatial resolution (horizontal, degree)	0.1	0.1	0.1	0.1	point	0.1	0.1	0.1	0.25	0.1
Species										
NO _x	X	X	X	X	X	X	X	X	X	X
SO ₂	X	X	X	X	X	X	X	X	X	X
CO	X	X	X	X	X	X	X	X	X	X
NMVOC	X	X	X	X	X	X	X	X	X	X



172

173 **Table 3. Anthropogenic | Open biomass^a emissions of MIXv2 by Asian countries and regions in 2017.**

Country	NO _x ^b	SO ₂	CO	NMVOC	NH ₃	PM ₁₀	PM _{2.5}	BC	OC	CO ₂ ^b
China^c	22.37 0.22	10.62 0.02	137.02 4.40	29.36 1.66	9.18 0.08	10.20 0.41	7.65 0.35	1.26 0.03	2.09 0.17	11.34 0.07
Japan	1127.0 8.4	274.8 1.5	2543.1 192.0	927.1 141.2	397.7 2.9	84.3 30.1	40.7 19.6	14.9 1.3	7.5 11.9	785.9 3.4
Korea, DPR	194.6 3.5	83.8 0.7	2580.5 92.7	140.4 61.7	107.4 1.6	96.6 13.5	52.6 9.3	10.0 0.6	16.4 5.4	29.7 1.5
Korea, Republic of	979.1 2.8	266.7 0.5	522.1 61.0	917.1 44.5	292.5 0.9	127.6 9.5	64.5 6.2	11.2 0.4	31.3 3.7	581.9 1.1
Mongolia	125.5 28.3	124.9 7.8	1057.9 945.5	50.3 368.7	196.1 17.6	45.5 129.7	20.6 110.3	2.7 4.2	3.5 62.7	18.3 14.2
Other East Asia^{cd}	2.43 0.04	0.75 0.01	6.70 1.29	2.03 0.62	0.99 0.02	0.35 0.18	0.18 0.15	0.04 0.01	0.06 0.08	1.42 0.02
India^c	9.34 0.11	13.82 0.01	61.23 1.91	14.46 1.23	9.87 0.03	7.20 0.27	4.97 0.18	0.86 0.01	1.72 0.09	2.88 0.04
Afghanistan	83.2 0.2	45.0 0.0	560.2 2.7	131.2 1.4	320.3 0.0	39.9 0.4	30.7 0.3	8.3 0.0	12.1 0.1	11.1 0.1
Bangladesh	342.3 2.8	224.5 0.3	3074.5 41.9	836.0 15.7	922.5 0.5	685.6 5.8	350.1 4.4	43.6 0.2	114.3 2.0	127.7 0.9
Bhutan	0.8 1.0	0.5 0.4	31.5 30.0	6.4 14.8	2.8 0.3	13.6 5.9	5.1 4.3	0.4 0.2	1.2 3.1	0.8 0.6
Maldives	0.6 0.0	0.3 0.0	1.3 0.0	0.5 0.0	0.0 0.0	0.0 0.0	0.0 0.0	0.0 0.0	0.0 0.0	0.1 0.0
Nepal	70.6 7.0	61.2 2.2	2143.1 189.7	483.5 94.9	263.8 1.9	238.0 36.5	159.6 26.5	24.3 1.1	79.1 19.1	42.8 3.6
Pakistan	638.7 6.7	1607.7 0.6	9000.4 133.3	2134.7 126.9	1890.5 2.7	1479.4 16.5	914.0 8.9	108.6 1.0	327.6 3.3	308.8 2.2
Sri Lanka	205.0 2.2	84.7 0.2	1356.4 31.2	390.7 21.3	99.6 0.5	144.5 4.0	101.0 2.8	19.0 0.2	46.8 1.0	39.5 0.7
Other South Asia^{ce}	1.34 0.02	2.02 0.00	16.17 0.43	3.98 0.27	3.50 0.01	2.60 0.07	1.56 0.05	0.20 0.00	0.58 0.03	0.53 0.01
Brunei	9.4 0.1	2.7 0.0	24.8 1.9	26.5 0.4	1.4 0.0	4.6 0.2	1.7 0.1	0.1 0.0	0.1 0.1	4.3 0.0
Cambodia	74.2 189.7	78.7 16.7	1155.5 2899.1	230.1 943.7	85.2 34.2	170.0 397.9	87.9 301.7	9.8 16.7	33.3 133.5	26.3 62.7
Indonesia	2560.0 86.3	3260.5 9.2	16039.6 2439.6	5438.5 559.2	1848.0 26.4	1258.0 264.6	839.1 188.3	136.5 8.9	338.5 97.1	619.0 36.6
Laos	61.4 115.8	126.2 10.0	296.3 1641.4	55.5 569.9	69.5 18.4	93.7 224.4	39.7 173.2	3.2 9.5	9.2 74.0	20.0 36.9



Malaysia	627.1 8.6	250.3 0.8	1234.6 167.2	1029.2 65.9	237.2 2.1	226.7 20.5	137.0 14.5	14.4 0.9	13.7 6.6	224.7 3.0
Myanmar	185.5 233.3	315.9 23.4	3168.3 3576.8	936.1 1280.0	679.1 40.6	292.3 510.1	206.2 387.9	32.3 20.7	104.2 182.8	68.3 78.0
Philippines	881.4 10.1	974.2 0.8	3705.7 139.1	1031.0 91.8	469.9 1.9	315.8 18.0	197.5 12.7	39.7 0.9	61.4 4.7	159.0 3.0
Singapore	78.0 0.0	74.8 0.0	55.4 0.1	286.8 0.1	4.4 0.0	77.0 0.0	60.8 0.0	0.9 0.0	0.3 0.0	44.7 0.0
Thailand	1081.5 72.7	337.3 6.1	5073.4 1056.3	1546.1 585.4	631.0 14.3	522.8 139.3	367.1 199.7	45.5 6.6	119.5 39.9	328.2 22.6
Vietnam	546.8 44.1	517.0 3.7	6224.7 664.2	1335.1 364.1	734.0 9.2	671.9 87.7	390.1 62.2	54.3 4.2	143.0 25.3	274.5 13.9
Southeast Asia^c	6.11 0.76	5.94 0.07	36.98 12.59	11.91 4.46	4.76 0.15	3.63 1.66	2.33 1.24	0.34 0.07	0.82 0.56	1.77 0.26
Asia (2017)^e	41.61 1.15	33.16 0.12	258.22 20.61	61.79 8.24	28.32 0.29	24.00 2.59	16.69 1.97	2.71 0.12	5.28 0.93	17.95 0.40
Asia (2010/2017) ^f	1.04 1.56	1.32 1.55	1.20 1.49	0.89 1.36	0.96 1.39	1.21 1.61	1.23 1.61	1.17 1.52	1.25 1.64	0.86 1.58
Asia (2011/2017)	1.10 1.33	1.39 1.45	1.18 1.88	0.92 1.29	0.96 1.52	1.23 1.64	1.25 1.60	1.19 1.30	1.26 1.74	0.93 1.55
Asia (2012/2017)	1.12 1.65	1.39 1.86	1.17 2.22	0.95 1.62	0.98 1.87	1.23 2.02	1.24 1.98	1.19 1.62	1.25 2.16	0.96 1.88
Asia (2013/2017)	1.09 1.49	1.32 1.59	1.15 1.89	0.96 1.42	1.00 1.65	1.19 1.78	1.21 1.74	1.17 1.53	1.21 1.87	0.96 1.67
Asia (2014/2017)	1.04 2.51	1.21 2.85	1.10 4.18	0.98 2.39	1.00 3.17	1.13 3.44	1.14 3.31	1.11 2.45	1.16 3.72	0.97 3.15
Asia (2015/2017)	1.01 3.05	1.12 3.72	1.06 6.36	0.97 3.08	1.01 4.46	1.05 4.73	1.07 4.49	1.05 2.85	1.09 5.22	0.97 4.25
Asia (2016/2017)	0.99 1.28	1.05 1.28	1.01 1.32	0.98 1.27	1.01 1.25	1.00 1.36	1.01 1.32	1.01 1.27	1.04 1.35	0.97 1.31

174

175 ^a Anthropogenic sector includes power, industry, residential, transportation and agriculture. Open biomass represents the “Open Biomass Burning” sector.

176 ^b Tg yr⁻¹ for CO₂, Gg yr⁻¹ for other species.

177 ^c Bold values are with the following units: Pg yr⁻¹ for CO₂, Tg yr⁻¹ for other species.

178 ^d Other East Asia represents East Asia other than China.

179 ^e Other South Asia represents South Asia other than India.

180 ^f Asia (year/2017) represents the ratio of emissions (year) to emissions (2017) for all of Asia within the MIXv2 domain.



181

Table 2. Sector and subsectors included in MIXv2^a.

Sector	Subsector	IPCC code ^b
Power	Power plants	1A1a
Industry	Industrial coal combustion	1A2, 1A1c
	Industrial other fuel combustion	1A2
	Chemical industry	1B2b, 2B
	Oil production, distribution, and refinery	1B2a
	Other industrial process	2A1, 2A2, 2A7, 2C, 2
	Industrial paint use	3A
	Solvent use other than paint	3B, 3C
Residential	Residential coal combustion	1A4b
	Residential biofuel combustion	1A4bx
	Residential other fuel combustion	1A4b
	Waste treatment	6A, 6C
	Domestic solvent use	3C
Transportation	On-road gasoline	1A3b
	On-road diesel	1A3b
	Off-road diesel	1A3c, 1A4c
Agriculture	Livestock	4B
	Fertilizer use	4D
Open biomass burning	Agriculture in-field burning	4F
	Fires	4E, 5A, 5C, 5D
Shipping	Domestic shipping	1A3d
	International shipping	1C2

182

^a Detailed source profiles assigned to sources within each subsector are summarized in Table S1.

183

^b Reference report: https://www.ipcc.ch/report/ar6/wg3/downloads/report/IPCC_AR6_WGIII_FOD_AnnexII.pdf

184

185 **2.3 Components of regional emission inventory**

186 **REASv3 for Asia.**

187 We used anthropogenic emissions from REASv3.3 developed by ACAP (Asia Center for Air
 188 Pollution Research) and NIES (National Institute for Environmental Studies) to fill the gaps
 189 where local inventories are not available. REASv3 was developed as a long historical emission
 190 inventory for Asia from 1950 - 2015 with monthly variations and relatively high spatial
 191 resolution (0.25 degree). Compared to previous versions, REASv3 updated the emission factors
 192 and information on control policies to reflect the effect of emission control measures, especially



193 for East Asia. Large power plants are treated as point sources and assigned with coordinates of
194 locations. In REASv3, power plants constructed after 2008 with generation capacity larger than
195 300 MW are added as point sources. Additionally, REASv3 updated the spatial and temporal
196 allocation factors for the areal sources. Emissions of Japan, the Republic of Korea and Taiwan
197 are originally estimated in the system. The REASv3 data were further developed to 2017
198 following the same methodology as Kurokawa et al. (2020) and updated to a finer spatial
199 resolution of 0.1 degree except for NH₃ emissions from fertilizer application where grid
200 allocation factor for 0.1 degree were prepared from that of 0.25 degree for REASv3.2.1 assuming
201 homogeneous distribution of emissions in each 0.25-degree grid cell. We used the REAS
202 estimates for Taiwan directly and replaced REAS with local inventories as illustrated below.

203

204 **MEICv2 for China.**

205 For China, we used the anthropogenic emissions from the MEIC model developed and
206 maintained by Tsinghua University. MEIC uses a technology-based methodology to quantify air
207 pollutants and CO₂ from more than 700 emitting sources since 1990 (Li et al., 2017b).
208 Specifically, MEIC has developed a unit-based power plant database, a comprehensive vehicle
209 modeling approach and a profile-based NMVOC speciation framework. Detailed methodology
210 and data sources can be found in previous MEIC studies (Li et al., 2017b; Liu et al., 2015; Zheng
211 et al., 2014). In version 2.0, iron and steel plants, and cement factories are also treated as point
212 sources, which is important to improve industrial emissions estimation (Zheng et al., 2021).
213 MEIC is an online data platform publicly available to the community for emissions calculation,
214 data processing and data downloading. MEIC delivers monthly emissions at various spatial
215 resolutions and chemical mechanisms as defined by the user. We downloaded the emissions at
216 0.1 degree generated from MEIC v2.0 and aggregated it to five anthropogenic sectors: power,
217 industry, residential, transportation and agriculture. We followed the speciation framework in the
218 MEIC model and applied it to other regions of Asia, as described in detail in Sect. 2.4. MEIC
219 emissions of SAPRC99, SAPRC07 and CB05 were used directly in MIX.

220

221 **PKU-NH₃ for NH₃, China.**

222 We replaced MEIC with the high-resolution PKU-NH₃ inventory for NH₃ emissions in China
223 developed by Peking University (Huang et al., 2012b; Kang et al., 2016). PKU-NH₃ uses a
224 process-based model to compile NH₃ emissions with emission factors that vary with ambient
225 temperature, soil property, and the method and rate of fertilizer application (Huang et al., 2012b).
226 Compared to the previous version used in MIXv1, PKU-NH₃ further refined emission factors by
227 adding the effects of wind speed and in-field experimental data of NH₃ flux in northern China
228 cropland. Emissions are allocated to 1km × 1km grids using spatial proxies derived from a land
229 cover dataset, rural population, etc (Huang et al., 2012b). Monthly emissions over China,
230 including Hong Kong, Macao, and Taiwan are available from 1980 to 2017. We aggregated the 9
231 sub-sectors into 5 MIX anthropogenic sectors (power, industry, residential, transportation,
232 agriculture) and excluded the agricultural in-field waste burning.



233

234 **ANL-India for power plants, India.**

235 ANL-India is a continuously-updated long-term power plant emission inventory for India
236 developed on a unit and monthly basis by Argonne National Laboratory (Lu and Streets, 2012;
237 Lu et al., 2011). Emissions are calculated for more than 1300 units in over 300 thermal power
238 plants based on the detailed information collected from various reports of the Central Electricity
239 Authority (CEA) in India. As much as possible, the accurate and actual operational data of power
240 units/plants are used in inventory development, including geographical locations, capacity,
241 commissioning and retirement time, actual monthly power generation, emission control
242 application, fuel type, source, specifications, and consumption, etc. Detailed method can be
243 found in Lu et al. (2011) and Lu and Streets (2012). ANL-India is available for NO_x, SO₂ and
244 CO₂. In this work, the 2010-2017 period of ANL-India at the monthly level is used directly in
245 MIX. We further merged ANL-India with REASv3 for other species to complete the emission
246 estimation in India. CO₂ emissions of ANL-India at 0.1°×0.1° grids were used to develop spatial
247 proxies by sectors, year, and month. Then, REASv3 emissions of all other species were re-
248 allocated to grids based on ANL derived spatial proxies. Although ANL-India provides
249 emissions by fuel type, the fuel heterogeneity of thermal power plants is not considered in the re-
250 gridding process of MIX here because about 93% of the thermal power generation in India
251 during 2010-2017 were fueled with coal (Lu and Streets, 2012).

252

253 **JPN (PM2.5EI and J-STREAM) for Japan.**

254 We used the JPN inventory to override the Japan emissions of REAS. JPN was jointly developed
255 by the Ministry of Environment, Japan (MOE-J) for mobile source emissions (i.e., PM2.5 EI)
256 and by the National Institute of Environmental Studies (NIES) for stationary source emissions (J-
257 STREAM). Major anthropogenic sources are included in PM2.5EI, with vehicle emissions
258 explicitly estimated in detail (Shibata and Morikawa, 2021). Emission factors are assigned as a
259 function of average vehicle velocity by 13 vehicle types and regulation years. The hourly
260 average vehicle type of trunk roads and narrow roads are obtained from in-situ measurements. In
261 addition to the running emission exhaust, emissions from engine starting, evaporation, tire ware,
262 road dust and off-road engines are also estimated. To keep consistency with the sector definition
263 of MIX, we excluded the road dust aerosol emissions and mapped other sources to five
264 anthropogenic sectors. For stationary sources, Japan emissions are derived from the Japan's
265 Study for Reference Air Quality Modeling (J-STREAM) model intercomparison project (Chatani
266 et al., 2020; Chatani et al., 2018). Long-term emissions of over 100,000 large stationary sources
267 are estimated based on energy consumption and emission factors derived from the emission
268 reports submitted to the government every three years (Chatani et al., 2020). NMVOC emissions
269 are speciated into SAPRC07 and CB05 using local source profiles. Emissions are distributed to
270 1km × 1km grids with monthly variations based on spatial and temporal proxies. We re-sampled
271 the monthly JPN emissions to 0.1°×0.1° grids and merged them into MIXv2.

272



273 **CAPSS for the Republic of Korea.**

274 For the Republic of Korea, we use the official emissions from CAPSS developed by the National
275 Institute of Environmental Research Center (Lee et al., 2011). CAPSS estimated the annual
276 emissions of air pollutants of CO, NO_x, SO_x, PM₁₀, PM_{2.5}, BC, NMVOCs and NH₃ based on the
277 statistical data collected from 150 domestic institutions since 1990s (Crippa et al., 2023). There
278 are inconsistencies on the long-term emissions trend of CAPSS due to data and methodology
279 changes over the time. We used the re-analyzed data of CAPSS during 2010-2017, which
280 updated the emission factors and added the missing sources. Point sources, area sources, and
281 mobile sources were processed using source-based spatial allocation methods (Lee et al., 2011).
282 Monthly variations by sectors are derived from REASv3 for the Republic of Korea and were
283 further applied to CAPSS. In MIXv2, the monthly gridded emissions allocated at 0.1-degree
284 grids for the anthropogenic sector (power, industry, residential, transportation, agriculture) of
285 CAPSS are integrated.

286

287 **GFEDv4s for open biomass burning, Asia.**

288 Emissions over Asia from GFEDv4s database with small fires were used as the default inventory
289 for open biomass burning sources. GFED quantified global fire emissions patterns based on the
290 Carnegie-Ames-Stanford Approach (CASA) biogeochemical model from 1997 onwards (van der
291 Werf et al., 2017). Compared to previous versions, higher quality input datasets from different
292 satellite and in situ data streams are used, and better parameterizations of fuel consumption and
293 burning processes are developed. We calculated emissions for trace gases, aerosol species and
294 CO₂ based on the burned biomass and updated emission factors by vegetation types provided by
295 the GFED dataset (Akagi et al., 2011; Andreae and Merlet, 2001). Monthly and daily emissions
296 were re-gridded from 0.25° to 0.1° and cropped to a unified domain as anthropogenic emissions.
297 Open fires of grassland, shrubland, savanna, forest, and agricultural waste burning are included.
298 We assigned profiles for each source category as listed in Table S1. Model-ready emissions of
299 SAPRC99, SAPRC07 and CB05 were lumped from individual species as described in Sect. 2.4.
300 GFED emissions are further replaced by PKU-Biomass over China.

301

302 **PKU-Biomass for biomass burning, China.**

303 China's emissions estimated by the PKU-Biomass inventory were used to override GFED
304 emissions for open biomass burning in MIXv2. PKU-Biomass is developed by Peking University
305 based on the MODIS fire radiative energy data for China from 1980 to 2017 (Huang et al.,
306 2012a; Song et al., 2009; Yin et al., 2019). Emission factors of both air pollutants and CO₂ are
307 assigned for four types of biomass burning types including forest, grassland, shrubland fires and
308 agricultural waste burning. PKU-Biomass takes account of the farming system and crop types in
309 different temperate zones. High-resolution emissions (1km) with daily variations are available.
310 We re-gridded emissions to 0.1° × 0.1° and aggregated the emissions to the "open biomass
311 burning" sector. An explicit source profile assignment approach was assigned to each vegetation



312 type. Emissions of three chemical mechanisms were further developed for PKU-Biomass and
313 merged into the MIXv2 final dataset over Asia.

314

315 **EDGARv6 for shipping, Asia.**

316 We used the shipping (domestic and international) emissions over Asia derived from EDGARv6
317 in MIXv2. EDGAR is a globally consistent emission inventory for anthropogenic sources
318 developed by the Joint Research Centre of the European Commission (Crippa et al., 2018;
319 Janssens-Maenhout et al., 2019). Emissions of both air pollutants and greenhouse gases are
320 estimated. EDGAR uses international statistics as activity data and emission factors varying with
321 pollutants, sector, technology, and abatement measures for emissions calculation for 1970-2018.
322 Shipping route data are used as spatial proxies to distribute emission estimates to 0.1-degree
323 grids. We downloaded the emissions data for both inland and international shipping from 2010 to
324 2017, processed the data to the MIX domain and aggregated them to the “Shipping” sector.
325 Monthly emissions are only available for 2018. We applied the monthly variations of air
326 pollutants in 2018 to emissions of 2010-2017 accordingly.

327

328 **2.4 NMVOC speciation**

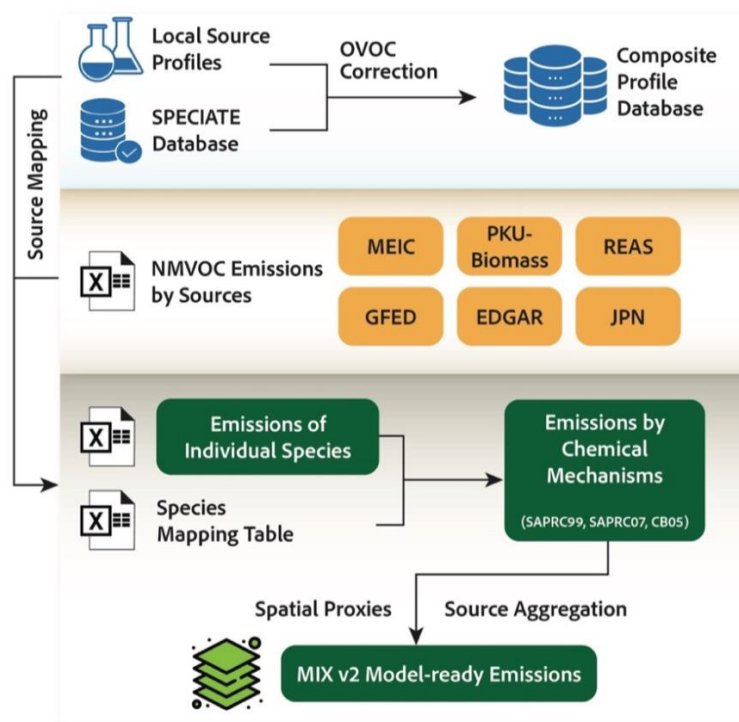
329 NMVOC speciation has substantial impacts on the model-ready emissions accuracy and
330 performance of chemical transport models (Li et al., 2014). Selection of profiles turns out to be
331 the most important contributor to uncertainties in emissions of individual species. To reduce the
332 uncertainties due to the inaccurate species mapping, Li et al. (2014) developed an explicit
333 assignment approach based on multiple profiles and mechanism-dependent mapping tables.

334 We processed the gas-phase speciation for NMVOCs following the profile-based mapping
335 procedure, as shown in Fig. 2. The speciation was conducted at a detailed source basis. Firstly,
336 we developed the composite source profile database by combining the US EPA’s SPECIATE
337 database v4.5 (last access: June 2019) (Simon et al., 2010) and available local measurements
338 (e.g., (Akagi et al., 2011; Mo et al., 2016; Xiao et al., 2018; Yuan et al., 2010). The complete list
339 of source profiles used in this work is provided in Table S1. To diminish the uncertainties due to
340 inappropriate sampling and analyses techniques regarding Oxygenated Volatile Organic
341 Compounds (OVOCs), we applied the OVOC correction to those incomplete profiles. The
342 detailed method can be found in previous studies (Li et al., 2014). Especially, the following
343 sources have significant OVOC emitted which should be addressed: coal combustion in
344 residential stoves (31%), residential wood and crop residue fuel use (23% ~ 33%) and diesel
345 engines (28% ~ 47%). Secondly, we assigned the composite profile database to each component
346 inventory to develop emissions of individual species. Lastly, individual species were lumped to
347 three chemical mechanisms (SAPRC99, SAPRC07, CB05) based on the conversion factors
348 derived from mechanism-dependent mapping tables (Carter, 2015).

349 For the Republic of Korea and Hong Kong, we applied the speciation factor for SAPRC99 and
350 CB05 by sectors developed from the SMOKE-Asia model, which have been used for MIXv1



351 (Woo et al., 2012). Emissions of SAPRC07 were further developed from SAPRC99 based on
352 Table S2, which applied MEIC speciated results.



353

354

355

356 2.5 Limitations

357 As a mosaic inventory, MIXv2 has several limitations when integrating various gridded products
358 into a unified dataset. Firstly, inconsistencies could exist at country boundaries where different
359 datasets were used for the adjacent countries (Janssens-Maenhout et al., 2015), for example, the
360 border between China and India. But limited effects are anticipated here given the small area
361 affected due to the high spatial resolution and the low population density at the border. Secondly,
362 extracting emissions by country from gridded maps may introduce uncertainties especially for
363 power plants located near the coast. This issue is more important because gridded emissions are
364 developed with higher spatial resolutions than earlier versions. Using an extended country map
365 by assigning extra adjacent grids of “ocean” with the neighboring country can reduce this bias.

366 It's always difficult to quantify the uncertainties for a mosaic emission inventory such as MIXv2.
367 The uncertainties for each of the component inventories are discussed in detail in corresponding
368 studies (Kang et al., 2016; Kurokawa and Ohara, 2020; Yin et al., 2019; Zheng et al., 2018).



369 Here we conducted uncertainty analyses qualitatively by comparing the MIXv2 estimates with
370 other bottom-up inventories and those derived from satellite retrievals in Sect. 4 (Li et al., 2018).

371

372 **3. Results and Discussions**

373 **3.1 Asian emissions in 2017**

374 In 2017, MIXv2 estimated emissions of Asia as follows: 41.6 Tg NO_x, 33.2 Tg SO₂, 258.2 Tg
375 CO, 61.8 Tg NMVOC, 28.3 Tg NH₃, 24.0 Tg PM₁₀, 16.7 Tg PM_{2.5}, 2.7 Tg BC, 5.3 Tg OC, and
376 18.0 Pg CO₂ for all anthropogenic sources including power, industry, residential, transportation
377 and agriculture. Emissions are summarized by Asian regions, including China, East Asia Other
378 than China (OEA), India, South Asia other than India (OSA) and Southeast Asia (SEA), as
379 shown in Table 3. China, India, and SEA together account for > 90% of the total Asian
380 emissions. China dominates the emissions (> 50%) of CO₂ (11.3 Pg, 63%), NO_x (22.4 Tg, 54%),
381 and CO (137.0 Tg, 53%), and contributes more than 30% to all other species. The contributions
382 of India are larger than 30% for SO₂ (13.8 Tg, 42%), NH₃ (9.8 Tg, 35%), BC (0.86 Tg, 32%),
383 OC (1.7 Tg, 33%), PM₁₀ (7.2 Tg, 30%), and PM_{2.5} (5.0 Tg, 30%). SEA ranks 3rd for all species,
384 including CO₂ (1.8 Pg, 10%), NO_x (6.1 Tg, 15%), SO₂ (5.9 Tg, 18%), NMVOC (11.9 Tg, 19%),
385 NH₃ (4.8 Tg, 17%), and ~15% of aerosol species. OEA's share varies from 1% (aerosol species)
386 to 8% (CO₂). Emission proportions of OSA are around 11% for NH₃, OC, and PM₁₀, and less
387 than 10% for others.

388 Sectoral contribution varies among species in Asia, according to our estimates. Power plants
389 contribute significantly to SO₂ (1st contributor, 38%) and CO₂ (2nd contributor, 33%). Industry
390 dominates the emissions of CO₂ (41%), NMVOC (44%), PM_{2.5} (39%), and PM₁₀ (47%). For
391 NO_x, transportation accounts for 33% of the total emissions, followed by industry (24%) and
392 inland and international shipping (18%). The residential sector contributes > 38% of emissions
393 for PM_{2.5}, BC, CO, and OC. NH₃ is dominated by agriculture (81%), followed by 13% from
394 residential.

395 Open biomass burning plays a key role in SEA and OEA's emissions budget, and is a minor
396 contributor for other regions, as shown in Table 3 and Figure 3. Including the open biomass
397 burning sector increases the emissions of OC, PM_{2.5}, PM₁₀, NMVOC, CO and CO₂, by 69%,
398 53%, 46%, 37%, 34% and 15%, respectively for SEA. Due to the active fire events, Southeast
399 Asia is the largest emission contributor for OC, PM₁₀, PM_{2.5} and NMVOC in 2014 and 2015.
400 Additionally, OEA has a significant emission increment for NMVOC (30%), OC (143%), PM₁₀
401 (52%) and PM_{2.5} (81%) when taking biomass burning into account. Given the large contributions
402 to ozone and climate change from NMVOC, CO and aerosols, it's important to address the open
403 biomass burning contributions in designing mitigation strategies for these areas.

404 In a global context, Asia shares out 43%~56% of the global anthropogenic emissions in 2017,
405 including 44% for NO_x, 43% for SO₂, 49% for CO₂, 51% for NH₃, 55% for CO, 50% for
406 NMVOC, and over 50% for all PM species (MIX for Asia, EDGAR for other regions). Figure S1
407 depicts the emissions trend by Asian regions, United States and OECD-Europe from



408 anthropogenic sources. Asia is playing a more and more important role in global climate change
409 as its CO₂ emission fraction has increased by 7% during 2010-2017. Especially, with the general
410 emission reductions in the U.S. and OECD-Europe, India and Southeast Asia is catching up with
411 the emissions of these two developed regions for NO_x, SO₂ and CO₂, and already surpassed their
412 emissions for other species. As of now, U.S. and OECD-Europe emissions are in general
413 comparable to those of OSA for most air pollutants.
414



415 3.2 Emissions evolution from 2010–2017

416 For anthropogenic sources, driven by stringent air pollution control measures implemented over
417 China and OEA since 2010, Asian emissions have declined rapidly by 24.3% for SO₂, 16.6% for
418 CO, 17.2% for PM₁₀, 18.7% for PM_{2.5}, 14.2% for BC and 19.8% for OC, according to our
419 estimates. On the contrary, CO₂, NMVOC and NH₃ still show emissions increasing continuously,
420 with growth rates of 16.5%, 12.6%, and 4.4% during 2010-2017, respectively. The emission
421 changing ratios are summarized in Table 3 and shown in Fig. 3 and Fig. 4. As demonstrated in
422 Fig. 4, power, industry, residential and transportation contribute to the rapid emission changes. In
423 contrast to the smooth patterns for anthropogenic trends, open biomass burning emissions vary
424 from year to year, peaking in 2015 as a result of El Niño (Field et al., 2016). Open fire activities
425 dominate the SEA emission changes for CO, OC, NMVOC, PM₁₀ and primary PM_{2.5} (see Fig.
426 3). Marked reductions are estimated for China, with a concurrent increase over India and
427 Southeast Asia for all species except CO₂, NMVOC and NH₃ (see Fig. 5). Consequently, air
428 pollutants, including ozone and secondary aerosol precursors of NO_x, have shifted southward
429 (Zhang et al., 2016). This changing spatial pattern has been confirmed from observations as
430 described in previous studies (Samset et al., 2019). We illustrate the driving forces of emissions
431 evolution for each species below. Shipping is not included in the following analyses.

432 **NO_x**. Power plants are the major driving factor for emissions reduction of NO_x (-3.5% from
433 2010-2017) during the investigated period. As illustrated by Zheng et al. (2018), China has
434 implemented very stringent emission standards for power plants since 2003, which has
435 continuous substantial impacts on SO₂, NO_x and particulate matters (Chinese National Standards
436 GB 13223-2003 and 3223-2011) (Zheng et al., 2018). Furthermore, “Ultra-low” emission
437 standards were set up by the Chinese government in 2015 to further reduce emissions from coal-
438 fired power plants by 60% by 2020. OEA shows 21% emissions decrease because of continuous
439 control measures over industry (-16%) and transportation (-32%). Due to insufficient control
440 strategies in India, OSA and SEA, NO_x anthropogenic emissions have grown by 38%, 18% and
441 19%, respectively, mainly driven by power plants and vehicle growth (see Fig. 5a). Open
442 biomass burning has limited effect (~11%) on NO_x emissions over SEA and is neglectable for
443 other regions (<3%).

444 **SO₂**. SO₂ emissions rapidly declined from 43.8 Tg to 33.1 Tg during 2010-2017, peaking in
445 2012. Significant reductions of industrial SO₂ emissions (-8.7 Tg, -39%) lead to the marked total
446 emissions decrease (see Fig. 4). China’s emissions dropped by 62%, partly offset by the
447 concurrent emissions increase of India (+46%) and Southeast Asia (+41%). Stringent control
448 measures shutting down small industrial boilers and cleaning larger ones in China are the
449 primary driving forces (Zheng et al., 2018). New emissions standards were set up for coal-fired
450 industrial boilers with tightened SO₂ limit values (Zheng et al., 2018). In addition, nationwide
451 phasing out of outdated industrial capacity and small, polluting units has been carried out in
452 China since 2013. Consequently, China’s emission fraction decreases from 64% to 32%, ranking
453 2nd in 2017. India’s proportion grew from 22% to 41%, and nowadays it’s the largest SO₂ emitter
454 in Asia (see Fig. 5b).



455 **CO.** Anthropogenic CO shows moderate emissions reduction (-16%) since 2010, driven by the
456 clean air actions implemented in China covering industry (-38% changes), residential (-20%) and
457 transportation (-22%). Based on the index decomposition analysis, the improvements in
458 combustion efficiency and oxygen blast furnace gas recycling in industrial boilers are the largest
459 contributors to the emission reductions in China (Zheng et al., 2018). Replacing polluted fuel
460 (biofuel, coal) with cleaner fuels (natural gas, electricity) is the primary driving force in the
461 residential sector. Despite the rapid vehicle growth which would typically yield a CO increase,
462 pollution control measures reduced the net CO emission factors by fleet turnover with cleaner
463 models replacing the older, more polluted vehicles in the market. OEA shows emission
464 reductions in industry (-37%), residential (-22%) and transportation (-28%). Residential fuel
465 combustion decreases by 20% and 11% for SEA and India, respectively, having a canceling
466 effect on the total emissions growth for these two regions. Open biomass burning accounts for
467 25% ~ 77% of CO emissions in SEA, which drives the total emissions reduction by 19% in 2017
468 compared to 2010. Additionally, the climate anomaly due to El Niño in 2015 leads to the rapidly
469 CO emissions drop from 2015 to 2016 in SEA.

470 **CO₂.** Driven by economic and population growth, anthropogenic CO₂ emissions show a rapid
471 increasing trend for China (15%), India (32%), OSA (32%) and SEA (21%). We found slight
472 emission decreases for OEA (-2%). Power, industry, and transportation grew by 28%, 12% and
473 35%, respectively, driving the total emissions increase continuously. In contrast, we estimated a
474 5% CO₂ emission reduction from the residential sector, attributed to reduced fossil fuel use.
475 Notable emissions have increased for sectors apart from residential for India (increasing rates
476 varying between 39% ~ 57%), OSA (43% ~ 56%), and SEA (9% ~ 48%). Fractions by regions
477 are stable during the studied period, with 62% contribution from China, 8% from OEA, 16%
478 from India, 3% from OSA, and 11% from SEA (see Fig. 3). Open biomass burning curbs the
479 total emission growth in SEA from +21% to +5%.

480 **NM_{VOC}.** Differing from the decreasing emission trend for NO_x, SO₂ and CO, NM_{VOC}
481 increases by 13% for anthropogenic, and 6% for all sources with open biomass burning. In
482 China, the industrial sector (+5.1Tg, +35%) is the major reason for the emissions growth, and
483 industrial solvent use (e.g., architecture paint use, wood paint use) is the largest contributor. The
484 share of solvent use rapidly rises from 28% in 2010 to 42% in 2017. In addition, oil production,
485 distribution and refineries, and chemical production lead to a corresponding emissions increase
486 by 44% (Li et al., 2019b). Due to fuel transfer in residential stoves and the effective pollution
487 control measures for on-road vehicles, China shows 18% and 22% emissions decreases,
488 respectively, slowing down the increasing trend. Industry and transportation drive the
489 anthropogenic emissions in India and SEA growing by 18% and 13%, respectively (see Fig. 5c).
490 In SEA, 64% of the total emissions are contributed by open biomass burning in 2015. Compared
491 to 2010, 2017 total emissions decreased by 12% in SEA, attributed to biomass burning.
492 NM_{VOC}s are speciated into three chemical mechanisms following the source-profile based
493 methodology (see Sect. 2.4). We analyzed the speciation results in Sect. 3.5.

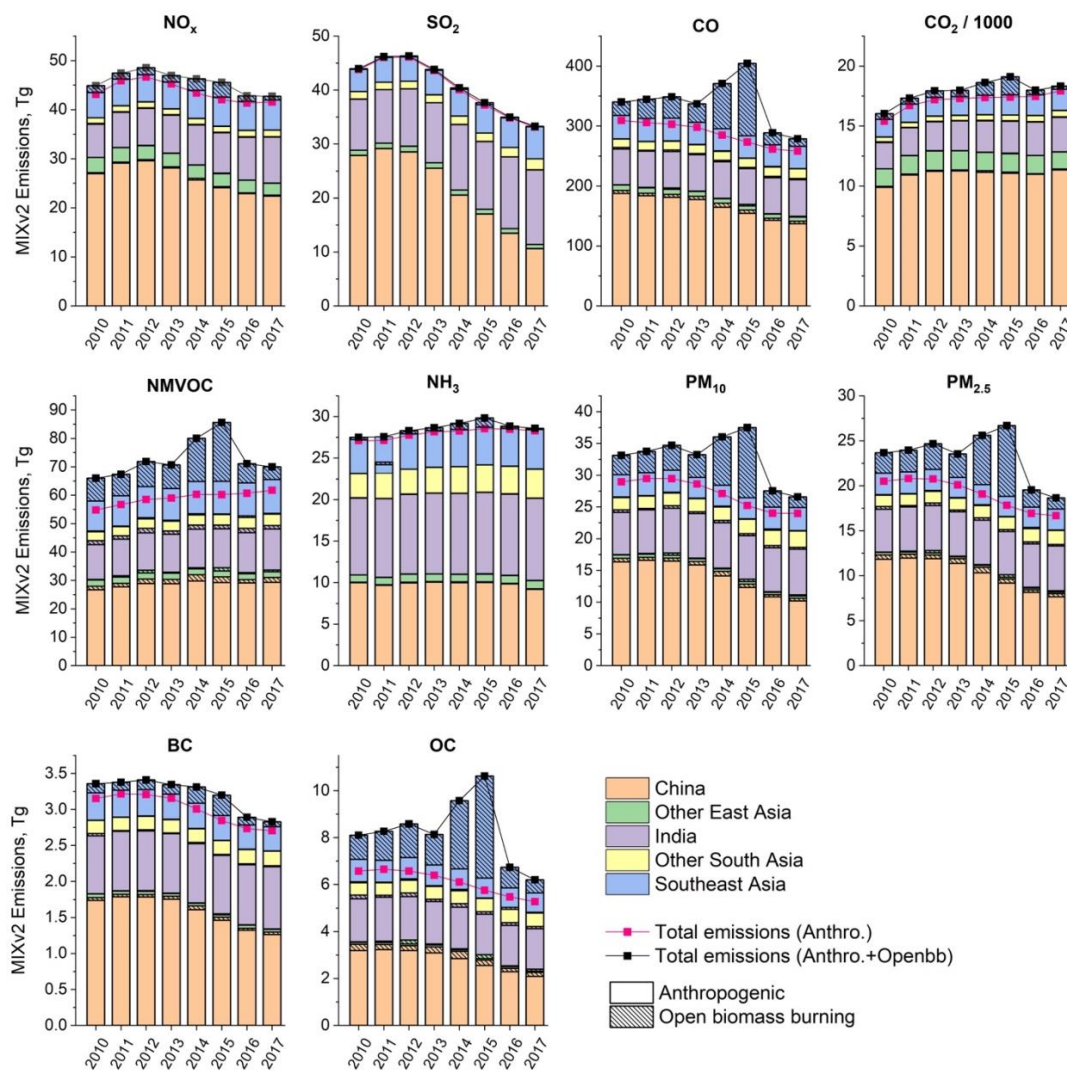
494 **NH₃.** As estimated by MIXv2, NH₃ emissions are generally flat, with slight increases (+4%) over
495 Asia due to the lack of targeted control measures. Over 80% of the total emissions are
496 contributed by fertilizer application and livestock manure. Transportation emissions in 2017 are



497 2.8 times greater than those in 2010 due to vehicle growth, which can play a key role for urban
498 air quality. India is the largest contributor (35%), followed by China (32%) and SEA (17%) (see
499 Fig. 3). India and OSA emissions show monotonic 7% and 20% increases, respectively.
500 According to our estimates, China decreases by 8% reflecting the agricultural activity rate
501 changes. Limited effects are estimated from open fires over NH₃ emissions budget, peaking at
502 19% of the total in 2015 for SEA.

503 **Particulate Matter (PM).** PM emissions are estimated to have decreased in Asia: -4.9 Tg PM₁₀ (-
504 17%), -3.8 Tg PM_{2.5} (-19%), -0.45 Tg BC (-14%), -1.3 Tg OC (-20%) for anthropogenic, and -
505 6.5 Tg PM₁₀ (-20%), -5.0 PM_{2.5} (-21%), -0.51 Tg BC (-15%), -1.9 Tg OC (-23%) after including
506 open biomass burning. Industrial and residential sectors are the primary driving forces of the
507 emissions reduction. The strengthened particulates standard for all emission-intensive industrial
508 activities, including iron and steel making, cement, brick, coke, glass, chemicals, and coal boilers
509 have driven the technology renewal and the phasing out of outdated, highly polluting small
510 facilities in China (Zheng et al., 2018). Reduction in fossil fuel use led to the residential emission
511 reduction of PM in China, India, and SEA. In China, pollution control measures reduced power
512 plant emissions by ~30% for PM₁₀, PM_{2.5} and BC, and counterbalanced the transportation
513 emissions despite vehicle ownership increasing by 270% in seven years. Other East Asia shows
514 significant anthropogenic emissions reduction for all PM species: -32% for PM₁₀, -33% for
515 PM_{2.5}, -27% for BC, and -31% for OC. Flat trends are estimated in India for all PM species
516 ($\pm 8\%$). Increasing industrial activities led to 24% - 35% emissions growth for PM₁₀ and PM_{2.5} in
517 OSA. As a result, China's emission fractions are shrinking, with growing contributions from
518 India and OSA (see Fig. 5d) for anthropogenic sectors. Taking PM_{2.5} as an example, the
519 emissions shares among Asian regions have changed significantly between 2010 and 2017: from
520 58% to 46% for China, 23% to 30% for India, and 12% to 14% for SEA (Fig. 5d). Open biomass
521 burning dominates the SEA emissions trend: -19% for PM₁₀, -24% for PM_{2.5}, -20% for BC, and -
522 30% for OC.

523



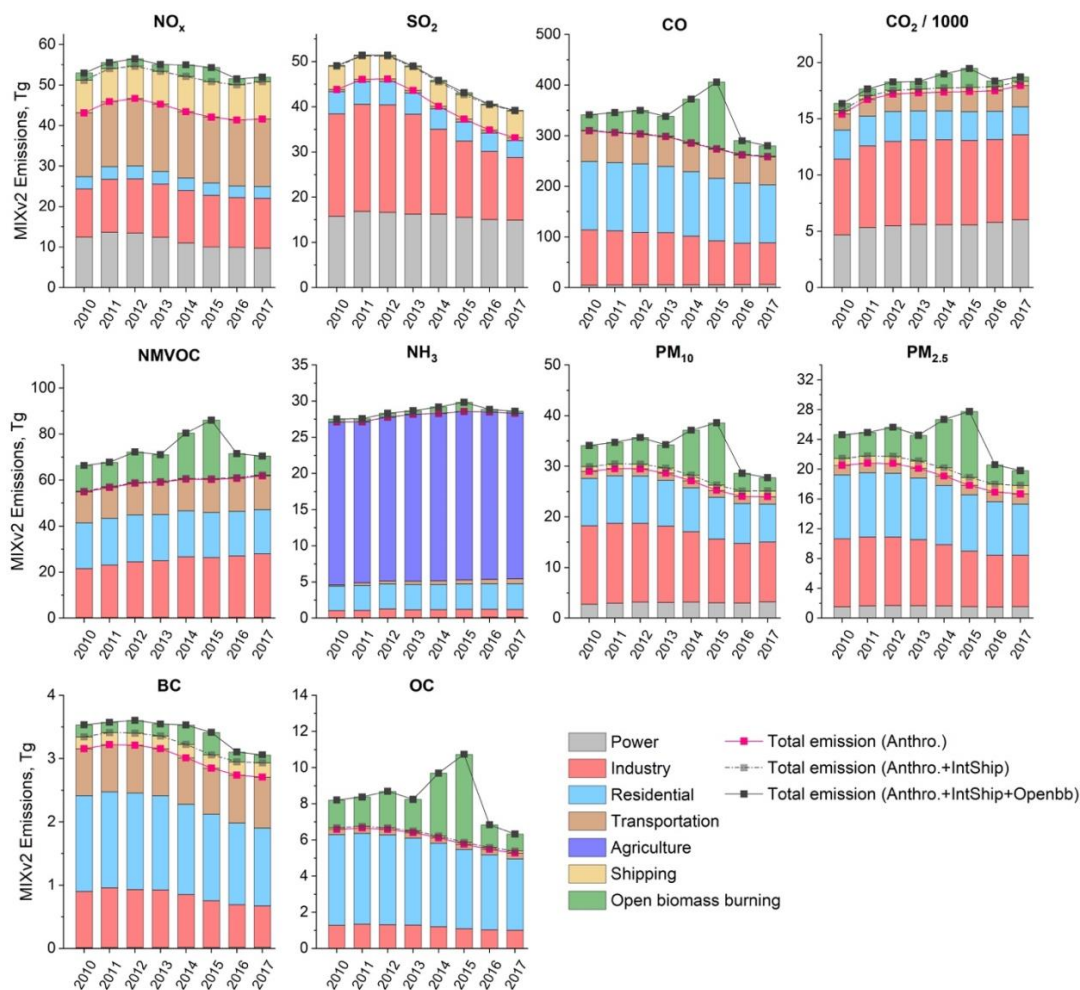
524

525

526

527

Figure 3. Emission changes by countries / regions from 2010 – 2017. Shares of open biomass burning for each region are shown as shadowed blocks.



528

529

530

531

532

533

534

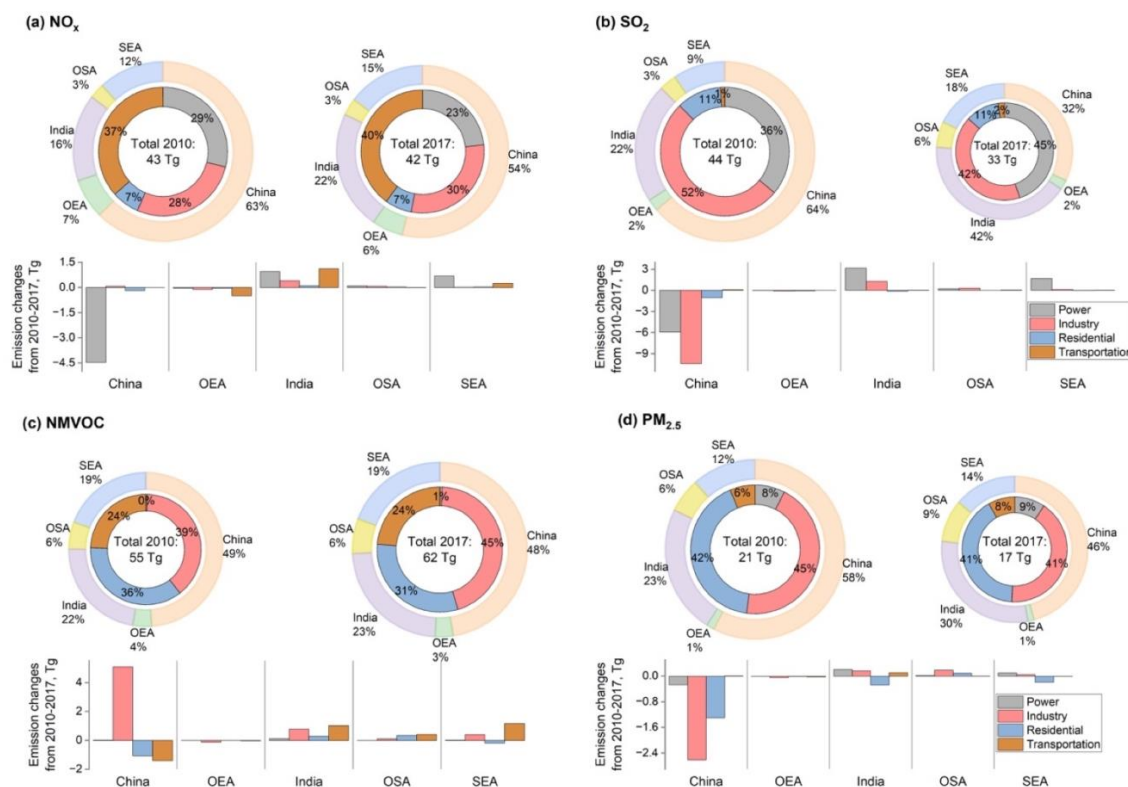
535

536

Figure 4. Emission changes by sectors in Asia from 2010 – 2017.



537



538

539

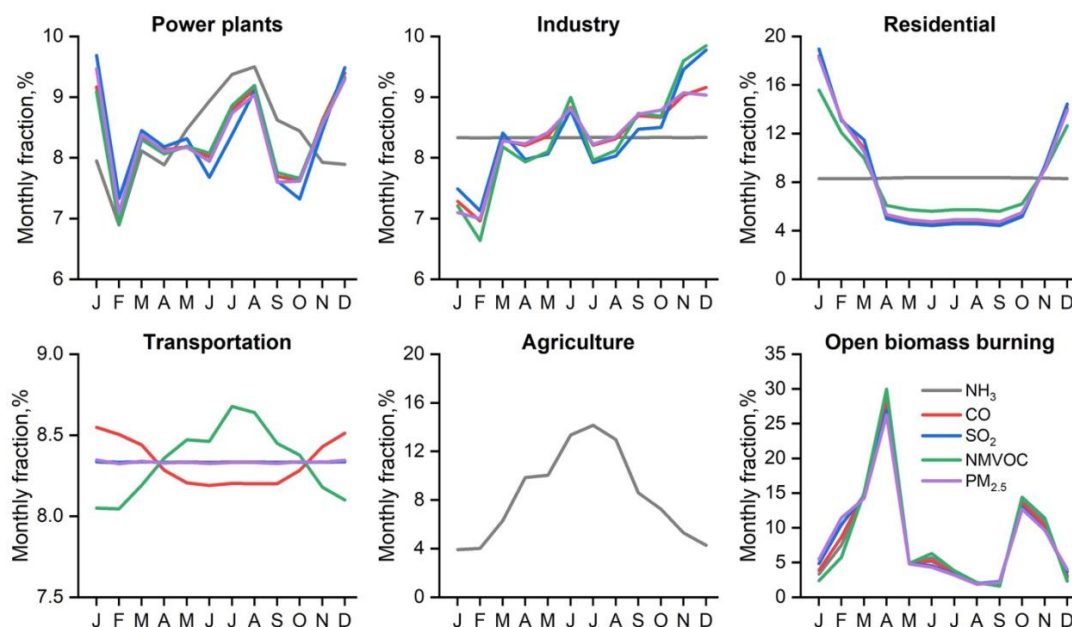
540

541

542

543

Figure 5. Emission changes for anthropogenic sources (power, industry, residential, and transportation) by regions and sectors from 2010 – 2017 for (a) NO_x, (b) SO₂, (c) NMVOC and (d) PM_{2.5}. The pie sizes are scaled with the total anthropogenic emissions in Asia. The unit for the total emission values in the center is Tg per year. OEA denotes East Asia other than China, OSA represents South Asia other than India, SEA is Southeast Asia.

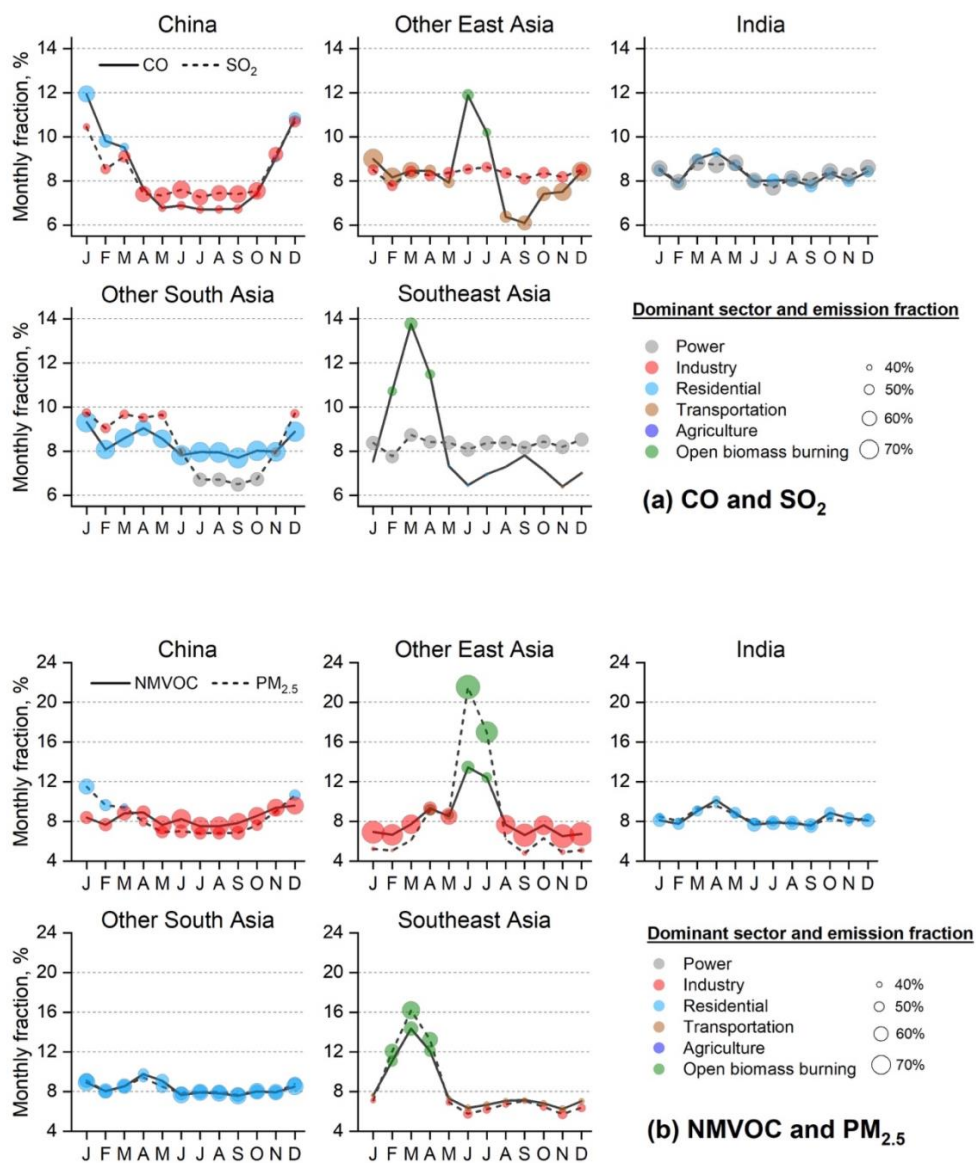


544

545

546

Figure 6. Monthly variations of emissions in Asia by sectors, 2017. For agriculture, only NH₃ emissions are estimated.



547

548

549

550

551

552

Figure 7. Monthly variations of emissions in Asian regions in 2017 for (a) CO (solid lines) and SO₂ (short, dashed lines), (b) NMVOC (solid lines) and PM_{2.5} (short, dashed lines). For each month, the dominant sector is labeled by circle color. Circle area is scaled based on the emission fraction of the dominant sector for each month. Both anthropogenic and open biomass burning are included.



553 3.3 Seasonality

554 Monthly variations of emissions are estimated in MIXv2, which are highly sector dependent.
555 Within the same sector, similar monthly emission variations are found among different species as
556 they are mainly driven by activity rates (see Fig. 6) (Li et al., 2017c). Figure 6 and Figure 7
557 illustrate the emission fractions by sectors, and the dominant sector (classified by circle color)
558 for each month for CO, SO₂, NMVOC and PM_{2.5} by regions in 2017, including both
559 anthropogenic and open biomass burning. Contribution of the “dominant sector” is scaled to the
560 circle area. Large circles represent the significant role of the dominant sector and small ones
561 (near 17%) indicate the balanced contribution from six sectors. The monthly emissions patterns
562 show large disparities varying with regions. Notable variations are estimated for emissions of
563 China, OEA and SEA. The residential sector of China is the largest contributor in winter for CO
564 and PM_{2.5}, leading to the “valley” curves. Industrial emissions show relatively high fractions in
565 the second half of the year aiming to achieve the annual production goal, which dominate the
566 emissions of SO₂, CO, NMVOC and PM_{2.5} for most of the months. The emissions peak in
567 summer for OEA and March for SEA are attributed to significant in-field biomass burning
568 activities. Indian and OSA emissions show relatively small monthly variations, compared to
569 other Asian regions. Thus, it’s important to take both anthropogenic and open biomass sectors
570 into account in seasonality analyses given their dominant roles varying by months, such as model
571 evaluations based on ground/satellite/aircraft measurements.

572

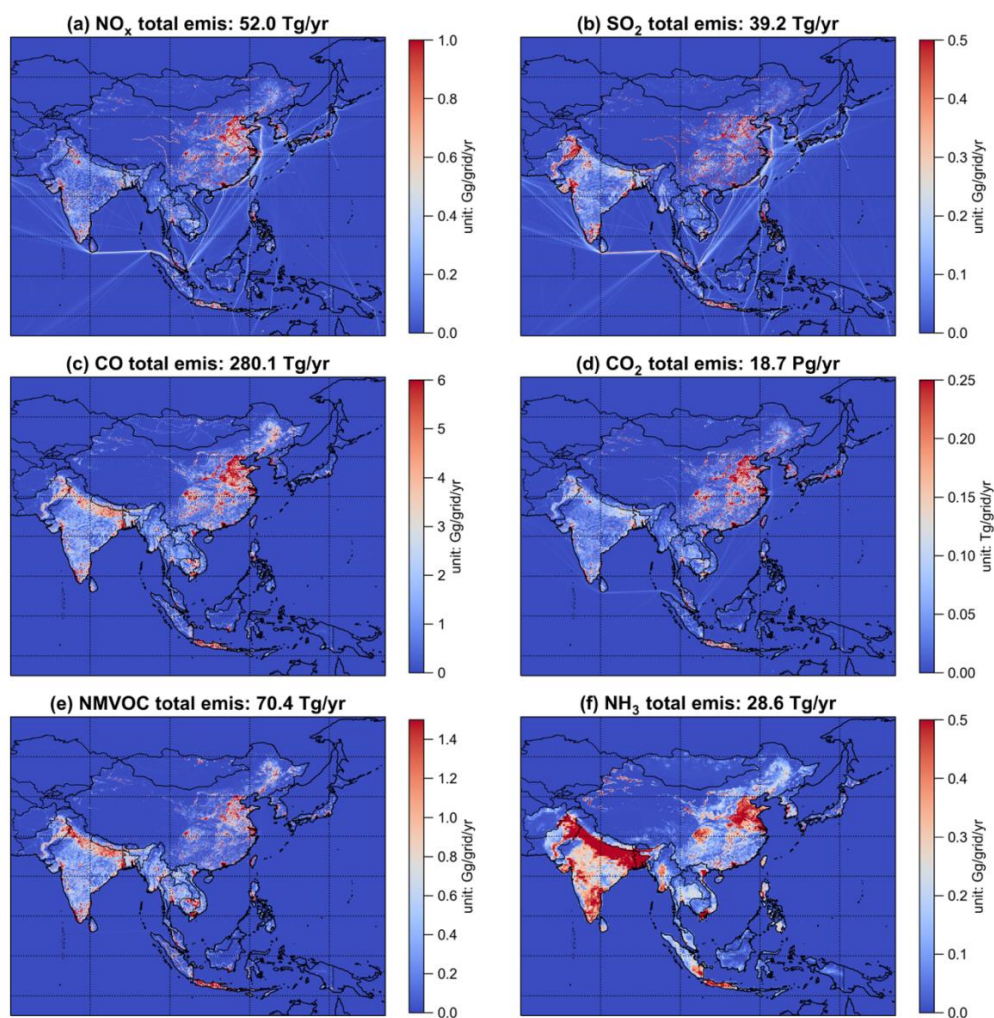
573 3.4 Spatial distribution

574 Gridded emissions at 0.1 × 0.1 degree were developed in our inventory. Power plant emissions in
575 China and India are developed on a unit basis and assigned with exact geophysical locations. For
576 other sources, emissions are allocated to grids based on spatial proxies, such as road map,
577 population, Gross Domestic Product (GDP), etc. The gridded MODIS fire product with high
578 spatial resolution (up to 1km) is the essential dataset for open biomass burning emission
579 estimation. Fig. 8 and Fig. 9 depict the spatial distribution of both CO₂ and air pollutants over
580 Asia in 2017, showing the distinct patterns of point source, roads, and city clusters. Emission
581 intensities of hot spots over the Indo-Gangetic Plain, spanning northern Pakistan, northern India
582 and Bangladesh are comparable to those of northern China and Indonesia, especially for NH₃,
583 NMVOC, BC and OC. Clear shipping routes can be seen for NO_x, SO₂, CO₂ and PM species.

584 Emission reductions in East Asia highlight the importance of air pollution control in Southern
585 Asia. We show the emission changes by latitude bands from 2010 to 2017 for ozone precursors
586 (NO_x, NMVOC, CO) and primary PM_{2.5} in Fig. 10 and Fig. S2. Largest reductions are estimated
587 between 35°N ~ 40°N for NO_x (-25%), CO (-32%) and PM_{2.5} (-35%) because of China’s
588 effective emission control strategies. On the other hand, NO_x anthropogenic emissions have
589 increased by 15% over 10°S ~ 0° (Southeast Asia), and +27% over 10°N ~ 20°N (driven by
590 India). Open biomass burning enlarged the emission amplitude for 15°S ~ 0° (Southeast Asia),
591 while had limited effect on the trends over other latitude bands (see Figure S2). To conclude,



592 NO_x has shifted southward in Asia. NMVOC emissions show generally increasing trend over all
593 latitude bands (+5% ~ +38%, anthropogenic). Differently, CO and primary $\text{PM}_{2.5}$ show general
594 emissions reduction since 2010 except over 15°S ~ 10°S and 10°N ~ 20°N. These latitudinal
595 shifts are of particular importance for the global tropospheric ozone budget as ozone precursors
596 emitted at low latitudes are more efficient at producing ozone than if the same quantity of
597 emissions is released at high latitudes (Zhang et al., 2016; Zhang et al., 2021).



598

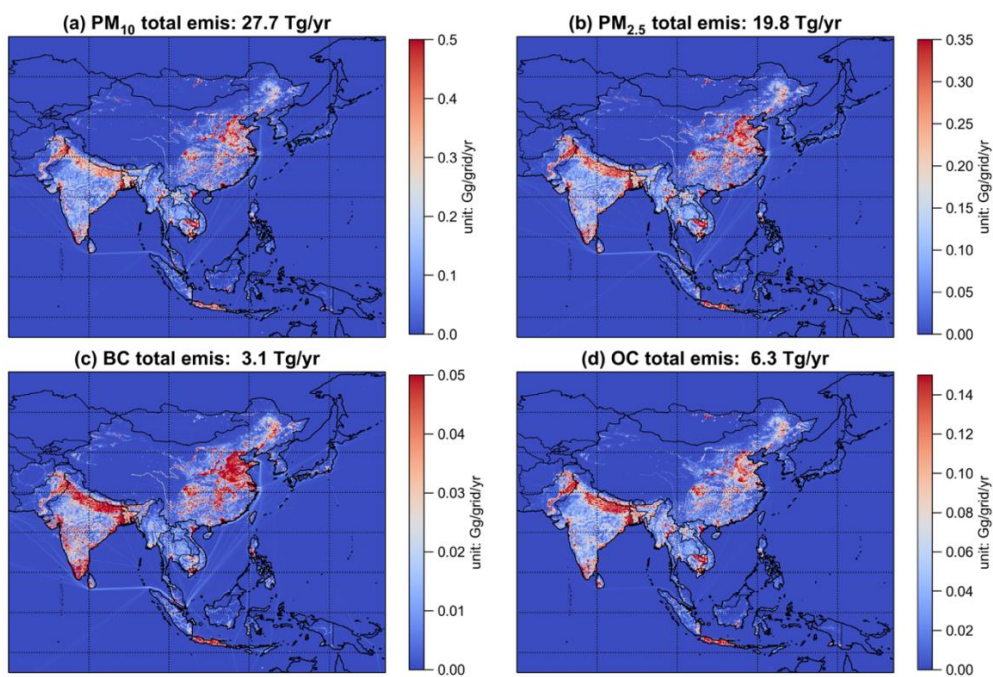
599

600

Figure 8. Spatial distribution of emissions in MIXv2 in 2017 for gaseous species.



601

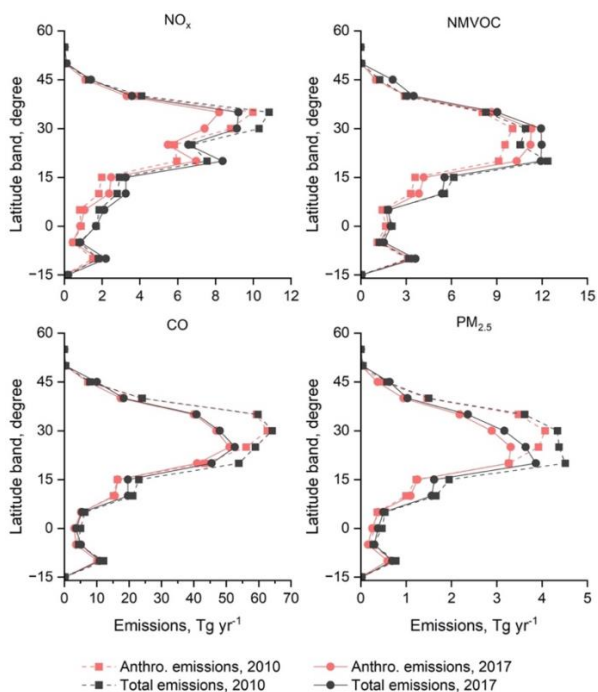


602

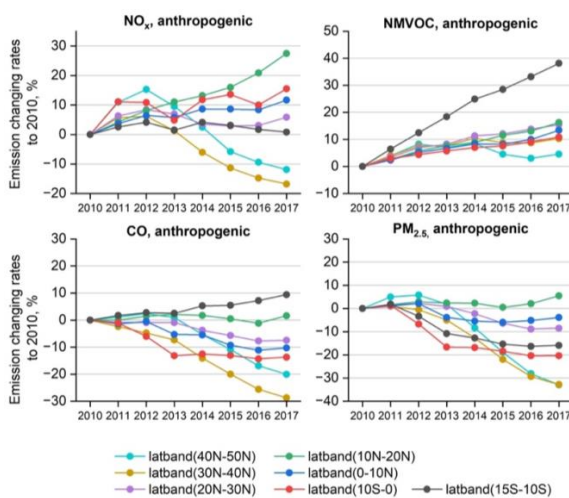
603

604

Figure 9. Spatial distribution of emissions in MIXv2 in 2017 for PM species.



(a)



(b)

605
606
607

608
609
610
611
612

Figure 10. Emissions in 2010 and 2017 (a), and anthropogenic emission changes from 2010 to 2017 (b) by latitude bands for NO_x, NMVOC, CO and PM_{2.5}. The total emissions trend by latitude (anthropogenic + open biomass burning) are shown in Figure S2.



613

614 **3.5 Speciated NMVOC emissions**

615 As one of the key precursors of ozone and secondary organic aerosols (SOA), NMVOC gain
616 more and more attention because of the emission increase due to relatively loose targeted control
617 measures. As estimated in MIXv2, Asian emissions have increased by 13% for anthropogenic
618 sources and 6% with additional open biomass burning. We speciated the total NMVOC to three
619 chemical mechanisms: SARPC99, SAPRC07 and CB05 following the profile-based approach
620 (Sect. 2.5). Emission changes during 2010-2017 by chemical groups are shown in Fig. 11.
621 Alkanes, Alkenes and Aromatics comprise 78% of the total emissions on a mole basis in 2017.
622 Driven by the growing activities in industry, emissions of Alkanes and Aromatics increased by
623 ~20% within 7 years, according to our estimates. Alkenes and Alkynes show flat trend as
624 combined results of emission reduction in residential, compensated by growth in industry and
625 transportation sectors. For OVOCs, especially Aldehydes, emissions decreased by 10% since
626 2010 due to reduced residential fuel combustion. Open biomass burning play a role over other
627 OVOCs (OVOCs other than Aldehydes and Ketones) emission changes. India, Southeast Asia,
628 and China are the largest contributors to the total Asian budget, with varying sector distributions
629 and driving forces by chemical groups.

630 Industry, mainly industrial solvent use, is the primary driving sector for emissions increase of
631 Alkanes (+15%) and Aromatics (+21%) in China. Moderate reductions are estimated for
632 anthropogenic OVOCs (-33% Aldehydes, +20% Ketones, -22% other OVOCs) attributed to fuel
633 transfer in the residential sector. OEA emissions show generally decreasing trends from -13%
634 (Ketones, Alkenes) to +3% (Alkynes) for anthropogenic sectors, and -10% (Ketones, Aromatics,
635 Others) to +25% (Other OVOCs) with additional open biomass burning. Industrial emissions
636 have decreased over all chemical groups for OEA. Similar sectoral distributions across chemical
637 species are found for India and OSA, dominated by the residential and transportation sectors.
638 More than 29% emissions growth are estimated for Alkanes and Aromatics, driven by industry,
639 residential, and transportation sectors in India and OSA. In SEA, ~20% increases are estimated
640 for emissions of Alkanes and Aromatics, and minor changes for Alkenes, Alkynes, Aldehydes
641 and Ketones (within 10%) during 2010-2017. OVOCs emissions in 2017 are 25% lower than the
642 values in 2010, contributed by residential sources and open biomass burning.

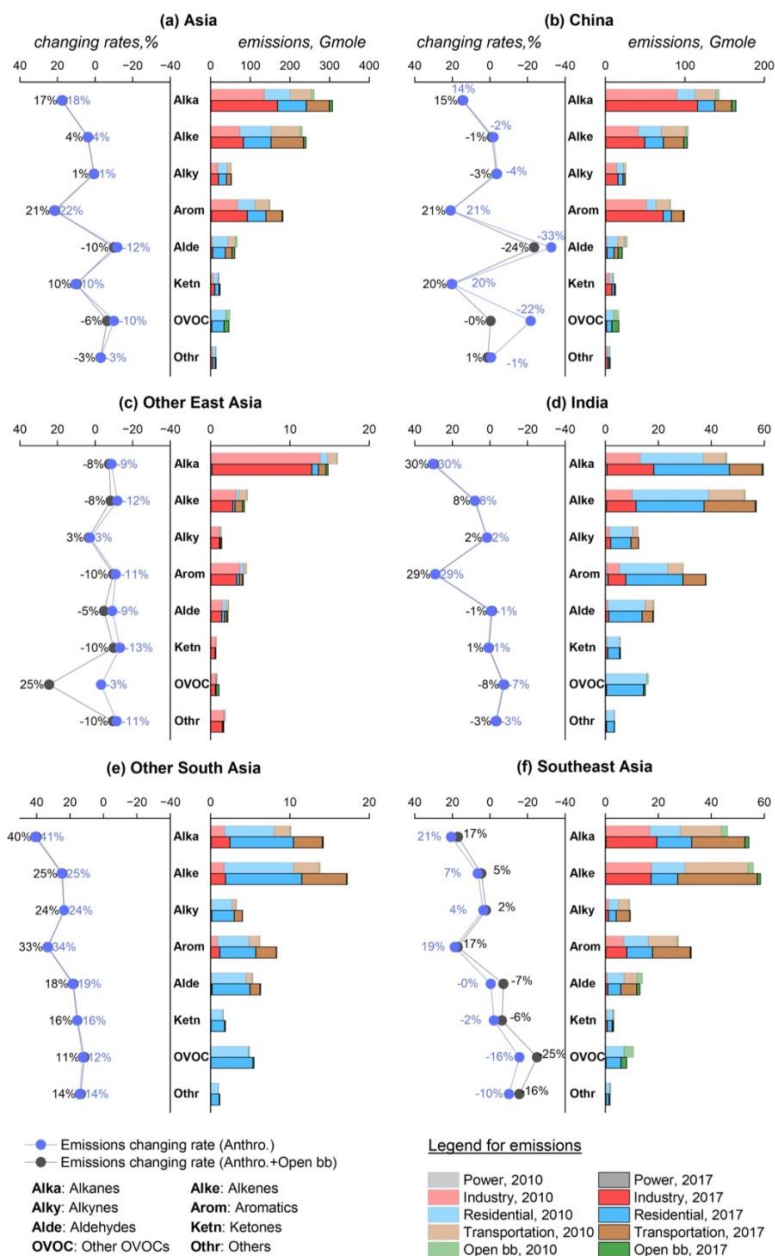
643

644

645

646

647



648

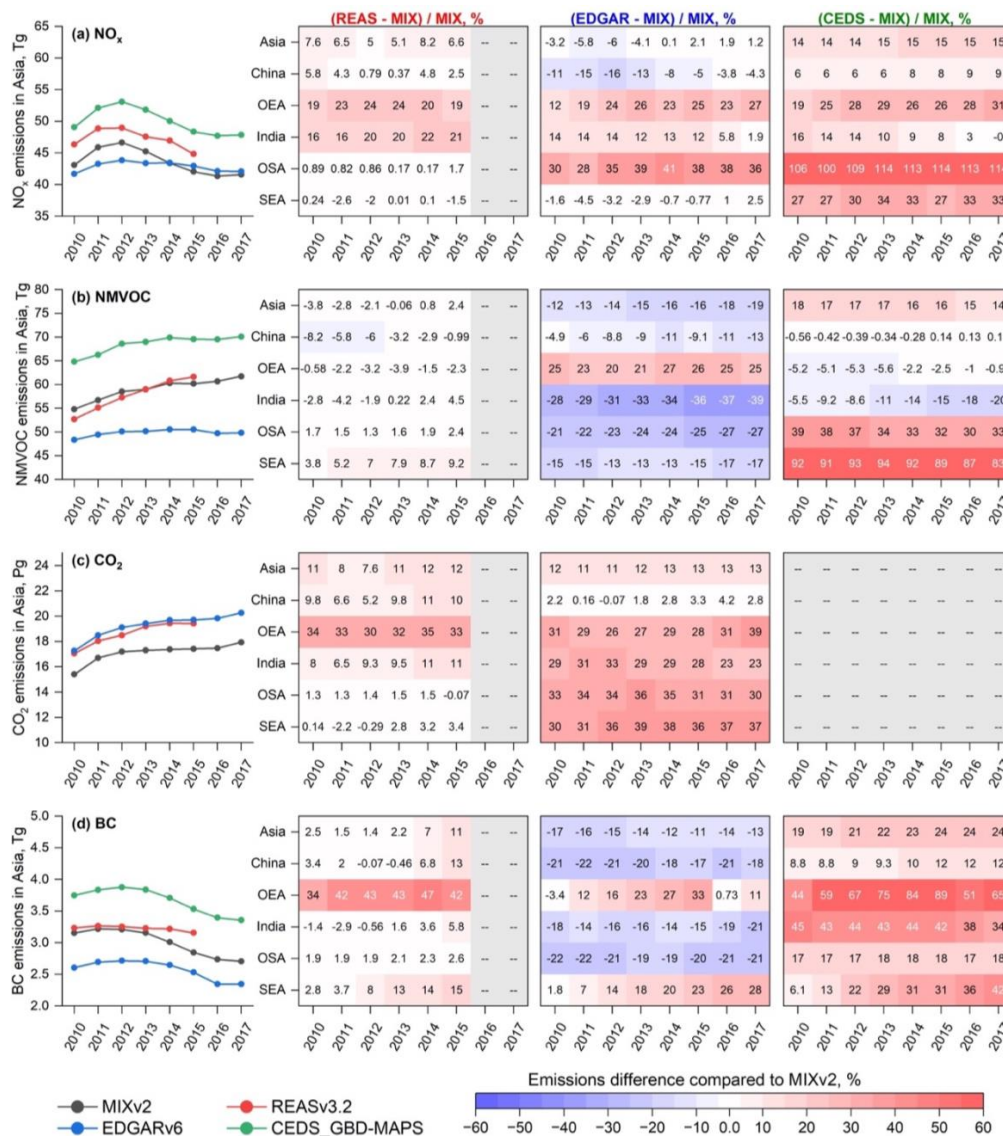
649

650

Figure 11. Emissions (right columns) and the emission changing rates from 2010–2017 (left columns) of NMVOCs by chemical groups. For each country/region, the left column



651 represents the emission changing rates (in unit of %), and the right column shows the
 652 emissions by sectors in 2010 and 2017. Chemical groups are lumped from the SAPRC07
 653 species following Table S3. Open bb denotes open biomass burning.



654

655

656

657

Figure 12. Emission comparisons between MIXv2, REASv3.2, EDGARv6, and CEDS_GBD-MAPs for (a) NO_x, (b) NMVOC, (c) CO₂ and (d) BC during 2010–2017 by Asian regions.



658 **4. Inter-comparisons with other bottom-up and top-down emission**
 659 **estimates**

660

661

Table 4. Top-down emission trends since 2010 over Asia.

Species	Estimates	Region	Period	AGR (% yr ⁻¹) ^a	Techniques
NO _x	Krotkov et al. (2016)	E China	2010-2015	-4.9	Satellite
	Liu et al. (2016)	E China	2010-2015	-5.1	Satellite
	Miyazaki et al. (2017)	China	2010-2016	-2.6	Inverse Modeling
	van der A et al. (2017)	E China	2010-2015	-1.7	Inverse Modeling
	Georgoulias et al. (2019)	China	2011-2018	-6.2	Satellite
	Hou et al. (2019)	China	2010-2017	-4.1	Satellite
	Itahashi et al. (2019)	China	2010-2016	-1.6	Inverse Modeling
	Zhang et al. (2019)	China	2010-2017	-5.0	Satellite
	MIXv2	China	2010-2017	-2.6	Bottom-up
	Krotkov et al. (2016)	India	2010-2015	3.4	Satellite
	Miyazaki et al. (2017)	India	2010-2016	2.5	Inverse Modeling
	Itahashi et al. (2019)	India	2010-2016	6.0	Inverse Modeling
	MIXv2	India	2010-2017	4.7	Bottom-up
	SO ₂	Tropospheric Chemistry Reanalysis (TCR-2) ^b	China	2010-2017	-7.1
Krotkov et al. (2016)		E China	2010-2015	-11.0	Satellite
van der A et al. (2017)		E China	2010-2015	-8.0	Inverse Modeling
C. Li et al. (2017)		China	2010-2016	-18.0	Inverse Modeling
Koukouli et al. (2018)		China	2010-2015	-6.2	Inverse Modeling
Zhang et al. (2019)		China	2010-2017	-4.0	Satellite
Qu et al. (2019) ^c		China	2010-2017	-4.0	Inverse Modeling
MIXv2		China	2010-2017	-12.9	Bottom-up
TCR-2 ^b		India	2010-2017	1.2	Inverse Modeling
Krotkov et al. (2016)		India	2010-2015	6.0	Satellite
C. Li et al. (2017)		India	2010-2016	3.4	Inverse Modeling
Qu et al. (2019) ^c		India	2010-2017	1.7	Inverse Modeling
MIXv2		India	2010-2017	5.6	Bottom-up
CO		Jiang et al. (2017) ^d	China	2010-2015	-2.8
	Zheng et al. (2019) ^e	China	2010-2017	-2.1	Inverse Modeling
	MIX v2	China	2010-2017	-4.4	Bottom-up
	Jiang et al. (2017) ^d	India / SEA	2010-2015	2.9	Inverse Modeling



	Zheng et al. (2019)	India	2010-2017	-1.7	Inverse Modeling
	MIXv2	India	2010-2017	0.4	Bottom-up
	Zheng et al. (2019)	SEA (an) ^f	2010-2017	-2.4	Inverse Modeling
	MIXv2	SEA (an)	2010-2017	-0.8	Bottom-up
	Jiang et al. (2017)	SEA (bb) ^g	2010-2014 [2010-2015] ^h	6.3 [51.6] ^h	Inverse Modeling
	Zheng et al. (2019)	SEA (bb)	2010-2017 [2010-2015]	-11.2 [40.1]	Inverse Modeling
	MIXv2	SEA (bb)	2010-2017 [2010-2015]	-7.9 [40.1]	Bottom-up
NMVO C	Stavrakou et al. (2017)	China	2010-2014	1.7	Inverse Modeling ⁱ
	Zhang et al. (2019)	China	2010-2017	1.0	Satellite ⁱ
	MIXv2	China	2010-2017	1.3	Bottom-up
NH ₃	Warner et al. (2017)	China	2010-2016	2.2	Satellite
	Damme et al. (2021)	China	2010-2017	5.5	Satellite
	MIXv2	China	2010-2017	-1.2	Bottom-up
	Damme et al. (2021)	India	2010-2017	0.5	Satellite
	MIXv2	India	2010-2017	2.2	Bottom-up
	Damme et al. (2021)	SEA	2010-2017 [2010-2015]	-2.7 [8.9]	Satellite
	MIXv2	SEA	2010-2017 [2010-2015]	1.7 [5.3]	Bottom-up

662

663 ^a AGR: Annual Growth Rate.

664 ^b Elguindi et al. (2020)

665 ^c Top-down estimates based on NASA products

666 ^d estimates derived from MOPITT profiles

667 ^e the results of full inversion # 3 are summarized here

668 ^f Southeast Asia for anthropogenic sources

669 ^g Southeast Asia for open biomass burning

670 ^h the growth rates between 2010 and 2015 are listed in square brackets because 2015 is a El Niño year

671 ⁱ HCHO columns are used

672

673 To provide potential uncertainty range of MIXv2, we compared our estimates with both regional
 674 and global inventories, as well as top-down estimates from previous satellite-based and inverse
 675 modeling studies. Figure 12 shows the emission comparisons of MIXv2 with REASv3.2,
 676 EDGARv6, and CEDS_GBD-MAPS (referred to as CEDS) (McDuffie et al., 2020) by Asian
 677 regions during 2010-2017 for NO_x, NMVOC, CO₂ and BC. REAS and MIX show the best
 678 agreement (differing within 12%) as expected because REAS was used as default estimates over
 679 Asia. Similar trends are found between REAS and MIX for all species except BC. The trends of
 680 NO_x in EDGAR are different than the others which peak in 2012, indicating the needs of re-
 681 visiting the parameterization of control policies in East Asia in the global inventory system.



682 EDGAR estimates are within 20% difference with MIX for the whole Asia, but with higher
683 discrepancies over OEA, OSA and SEA. NMVOCs are 12%~19% lower in EDGAR, mainly for
684 India and OSA. Notably, the emission discrepancies have grown larger in recent years, attributed
685 to the differences in emissions trends. EDGAR NMVOC emissions show a relatively flat trend,
686 in contrast to the continuously increasing pattern of MIX. Emissions of CO₂ over OEA, OSA and
687 SEA seem to be uncertain, with more than 30% difference between EDGAR and MIX. Similarly,
688 the increasing emission differences of BC in SEA needs to be noted when used in climate model
689 simulations. The emission trends of CEDS are consistent with those of MIX because MEIC was
690 applied to scale the emissions in the CEDS system (McDuffie et al., 2020). However, compared
691 to MIX, CEDS emissions are generally higher across regions and species, with large
692 discrepancies over OEA (+65% for BC, +31% for NO_x in 2017), India (+34% for BC), OSA
693 (+114% for NO_x, +33% for NMVOCs) and SEA (+33% for NO_x, +83% for NMVOCs, +42% for
694 BC). These comparisons highlight the potential uncertainties of bottom-up emission inventories
695 over South Asia and Southeast Asia where information is still limited compared to East Asia.
696 More validations and revisions are needed to identify the reasons of the discrepancies and close
697 the gaps between the different sources of estimates.

698 Table 4 summarizes the top-down emission annual growth rates since 2010 as derived from
699 satellite retrievals and inverse modeling studies. MIX trends show high consistency with the top-
700 down estimates, especially the inverse modeling results. Decreasing trends since the peak in
701 2012 for NO_x emissions in China are validated from space (Georgoulias et al., 2019; Hou et al.,
702 2019; Itahashi et al., 2019; Krotkov et al., 2016; Liu et al., 2016; Miyazaki et al., 2017; van der
703 A et al., 2017; Zhang et al., 2019). The annual growth rates derived directly from satellite
704 retrievals (-4.1 ~ -6.2 % yr⁻¹) are in general larger than those from inverse modeling (-1.6 ~ -
705 2.6 % yr⁻¹) which jointly account for the air transport and chemical non-linearity. Similar
706 declining trends are found from top-down estimates of SO₂ (Elguindi et al., 2020; Koukouli et
707 al., 2018; Krotkov et al., 2016; Li et al., 2017a; Qu et al., 2019; van der A et al., 2017; Zhang et
708 al., 2019) and CO (Jiang et al., 2017; Zheng et al., 2019) over China. For India, emissions have
709 been detected to grow continuously from space for NO_x and SO₂, with growth rates consistent
710 with the inventory estimation. Slightly increasing trend is detected from space for HCHO in
711 China, as an indicator of NMVOC emissions (Stavrakou et al., 2017; Zhang et al., 2019). 2015 is
712 an El Niño year, and this climate anomaly turns out to significantly affect the emissions trends of
713 CO and NH₃ in SEA (Van Damme et al., 2021). More inverse modeling work by combining
714 multiple species are needed for NH₃ over Asia to shed light on the uncertainty range of inventory
715 estimation.

716

717

718

719

720



721 5. Concluding remarks

722

723 In this work, we developed the MIXv2 emission inventory for Asia during 2010–2017 resolved
724 with relatively high spatial resolution (0.1°), temporal resolution (monthly) and chemical
725 speciation (SAPRC99, SAPRC07, CB05). MEICv2, PKU-NH₃, PKU-Biomass, ANL-India,
726 CAPSS, JPN are used to represent the best available emission inventories for China, India, the
727 Republic of Korea, and Japan, fill-gaped with REASv3 and GFEDv4. Constructing a long-term
728 mosaic emission inventory requires substantial international collaborations. MIXv2 was
729 developed based on the state-of-the-art updated emission inputs under the framework of MICS-
730 Asia Phase IV, and is now ready to feed the atmospheric chemistry models and improve
731 chemistry-climate models for long-term analyses. With high spatial resolution up to 0.1° , MIXv2
732 is capable of supporting model activities at regional and even local scales. As far as we know,
733 MIXv2 is the first mosaic inventory with both anthropogenic and open biomass burning
734 estimated by incorporating local emission inventories. Emissions are aggregated to seven sectors
735 in MIX: power, industry, residential, transportation, agriculture as anthropogenic sources, along
736 with open biomass burning and shipping. With three chemical mechanisms developed using a
737 consistent speciation framework, MIXv2 can be used in most of the atmospheric models even for
738 those configured with updates on ozone and secondary organic aerosols formation. MIXv2 also
739 has CO₂ emissions based on the same emissions model for 9 air pollutants (NO_x, SO₂, CO,
740 NMVOC, NH₃, PM₁₀, PM_{2.5}, BC, OC), providing a consistent dataset for climate-air quality
741 nexus research. Gridded monthly emissions are publicly available at
742 <https://csl.noaa.gov/groups/csl4/modeldata/data/Li2023/>.

743 Driving forces of the emission changes during 2010–2017 are investigated based on MIXv2.
744 Significant emission reductions from anthropogenic sources are found for SO₂, CO, PM₁₀, PM_{2.5},
745 BC, and OC, driven by effective clean air actions conducted over China and Other East Asia.
746 India, Other South Asia, and Southeast Asia show continuously increasing emissions trends since
747 2010, limiting the emissions reduction for Asia as a whole. On the contrary, NMVOC and NH₃
748 emissions increased or remained flat due to insufficient targeted control measures. Open biomass
749 burning is the largest contributor to Southeast Asia for emissions of CO, NMVOC and OC. NO_x
750 emissions have shown clear latitudinal shifts southward in Asia, which is important for global
751 tropospheric ozone budget. Our estimated trends are in general consistent with those derived
752 from satellite retrievals.

753 Further validation is needed for MIXv2 for better understanding of the data reliability. Inverse
754 modeling studies on NMVOC and NH₃ are still limited, partly attributed to the lack of available
755 measurement data over Asia. With the launch of the Geostationary Environment Monitoring
756 Spectrometer (GEMS) and the availability of hourly retrievals of atmospheric composition, top-
757 down constraints on both emissions spatial distributions and temporal variations are now
758 possible (Kim et al., 2020) on the scale of Asia. In-situ measurements, aircraft and satellite data
759 should be combined with inventory and model simulations to improve emission estimates in the
760 future.



761

762 **6. Data availability**

763 MIXv2 gridded monthly emissions data for 2010-2017 by 10 species and 7 sectors are available
764 at: <https://csl.noaa.gov/groups/csl4/modeldata/data/Li2023/>.

765

766 **7. Author contribution**

767 M. Li, Q. Zhang, J. Kurokawa and J. Woo initiated the research topic. M. Li developed the
768 emissions model, conducted the analyses, and prepared the paper. J. Kurokawa, Q. Zhang, J.
769 Woo, T. Morikawa, S. Chatani, Z. Lu, Y. Song, G. Geng, H. Hu, J. Kim provided the regional
770 emissions data. O. R. Cooper and B. C. McDonald have contributed by providing the computing
771 resources and data analyses. All co-authors have contributed with paper revision comments.

772

773 **8. Competing interests**

774 At least one of our co-authors are members of the editorial board of ACP.

775

776

777 **9. Acknowledgement**

778

779 MEIC has been developed and maintained by Tsinghua University, supported by the National
780 Key R&D program of China (grant no. 2022YFC3700605). REASv3 has been supported by the
781 Environmental Research and Technology Development Fund (grant nos. S-12 and S-20,
782 JPMEERF21S12012) of the Environmental Restoration and Conservation Agency of Japan and
783 the Japan Society for the Promotion of Science, KAKENHI (grant no. 19K12303). The ANL-
784 India emission inventory was partially funded by the National Aeronautics and Space
785 Administration (NASA) as part of the Air Quality Applied Sciences Team (AQAST) program
786 and by the Office of Biological and Environmental Research of Office of Science in the U.S.
787 Department of Energy in support of the Ganges Valley Aerosol Experiment (GVAX). Argonne
788 National Laboratory is operated by UChicago Argonne, LLC, under Contract No. DE-
789 AC02-06CH11357 with the U.S. Department of Energy. JPN emissions are developed by the
790 Environment Research and Technology Development Fund (grant nos. JPMEERF20222001,
791 JPMEERF20165001 and JPMEERF20215005) of the Environmental Restoration and
792 Conservation Agency provided by Ministry of the Environment of Japan, and the FRIEND (Fine

793



794 Particle Research Initiative in East Asia Considering National Differences) project through the
795 National Research Foundation of Korea (NRF) funded by the Ministry of Science and ICT (grant
796 no. 2020M3G1A1114622).

797 This compilation of the MIXv2 inventory has been supported by NOAA Cooperative Agreement
798 with CIRES, NA17OAR4320101 and NA22OAR4320151. The scientific results and
799 conclusions, as well as any views or opinions expressed herein, are those of the authors and do
800 not necessarily reflect the views of NOAA or the Department of Commerce.

801

802

803



804 **References**

805

- 806 Akagi, S. K., Yokelson, R. J., Wiedinmyer, C., Alvarado, M. J., Reid, J. S., Karl, T., Crounse, J.
807 D., and Wennberg, P. O.: Emission factors for open and domestic biomass burning for use in
808 atmospheric models, *Atmos. Chem. Phys.*, 11, 4039-4072, 2011.
- 809 Andreae, M. O. and Merlet, P.: Emission of trace gases and aerosols from biomass burning,
810 *Global Biogeochemical Cycles*, 15, 955-966, 2001.
- 811 Carter, W. P. L.: Development of a database for chemical mechanism assignments for volatile
812 organic emissions, *Journal of the Air & Waste Management Association*, 65, 1171-1184, 2015.
- 813 Chatani, S., Shimadera, H., Itahashi, S., and Yamaji, K.: Comprehensive analyses of source
814 sensitivities and apportionments of PM_{2.5} and ozone over Japan via multiple numerical
815 techniques, *Atmos. Chem. Phys.*, 20, 10311-10329, 2020.
- 816 Chatani, S., Yamaji, K., Sakurai, T., Itahashi, S., Shimadera, H., Kitayama, K., and Hayami, H.:
817 Overview of Model Inter-Comparison in Japan's Study for Reference Air Quality Modeling (J-
818 STREAM), *Atmosphere*, 9, 19, 2018.
- 819 Chen, L., Gao, Y., Zhang, M., Fu, J. S., Zhu, J., Liao, H., Li, J., Huang, K., Ge, B., Wang, X.,
820 Lam, Y. F., Lin, C. Y., Itahashi, S., Nagashima, T., Kajino, M., Yamaji, K., Wang, Z., and
821 Kurokawa, J.: MICS-Asia III: multi-model comparison and evaluation of aerosol over East Asia,
822 *Atmos. Chem. Phys.*, 19, 11911-11937, 2019.
- 823 Crippa, M., Guizzardi, D., Butler, T., Keating, T., Wu, R., Kaminski, J., Kuenen, J., Kurokawa,
824 J., Chatani, S., Morikawa, T., Pouliot, G., Racine, J., Moran, M. D., Klimont, Z., Manseau, P.
825 M., Mashayekhi, R., Henderson, B. H., Smith, S. J., Suchyta, H., Muntean, M., Solazzo, E.,
826 Banja, M., Schaaf, E., Pagani, F., Woo, J. H., Kim, J., Monforti-Ferrario, F., Pisoni, E., Zhang,
827 J., Niemi, D., Sassi, M., Ansari, T., and Foley, K.: The HTAP_v3 emission mosaic: merging
828 regional and global monthly emissions (2000–2018) to support air quality modelling and
829 policies, *Earth Syst. Sci. Data*, 15, 2667-2694, 2023.
- 830 Crippa, M., Guizzardi, D., Muntean, M., Schaaf, E., Dentener, F., van Aardenne, J. A., Monni,
831 S., Doering, U., Olivier, J. G. J., Pagliari, V., and Janssens-Maenhout, G.: Gridded emissions of
832 air pollutants for the period 1970–2012 within EDGAR v4.3.2, *Earth Syst. Sci. Data*, 10, 1987-
833 2013, 2018.
- 834 Elguindi, N., Granier, C., Stavrakou, T., Darras, S., Bauwens, M., Cao, H., Chen, C., Denier van
835 der Gon, H. A. C., Dubovik, O., Fu, T. M., Henze, D. K., Jiang, Z., Keita, S., Kuenen, J. J. P.,
836 Kurokawa, J., Liousse, C., Miyazaki, K., Müller, J. F., Qu, Z., Solmon, F., and Zheng, B.:
837 Intercomparison of Magnitudes and Trends in Anthropogenic Surface Emissions From Bottom-
838 Up Inventories, Top-Down Estimates, and Emission Scenarios, *Earth's Future*, 8,
839 e2020EF001520, 2020.
- 840 Field, R. D., van der Werf, G. R., Fanin, T., Fetzer, E. J., Fuller, R., Jethva, H., Levy, R.,
841 Livesey, N. J., Luo, M., Torres, O., and Worden, H. M.: Indonesian fire activity and smoke



- 842 pollution in 2015 show persistent nonlinear sensitivity to El Niño-induced drought, Proceedings
843 of the National Academy of Sciences, 113, 9204-9209, 2016.
- 844 Fiore, A. M., Naik, V., and Leibensperger, E. M.: Air Quality and Climate Connections, Journal
845 of the Air & Waste Management Association, 65, 645-685, 2015.
- 846 Gao, M., Han, Z., Liu, Z., Li, M., Xin, J., Tao, Z., Li, J., Kang, J. E., Huang, K., Dong, X.,
847 Zhuang, B., Li, S., Ge, B., Wu, Q., Cheng, Y., Wang, Y., Lee, H. J., Kim, C. H., Fu, J. S., Wang,
848 T., Chin, M., Woo, J. H., Zhang, Q., Wang, Z., and Carmichael, G. R.: Air quality and climate
849 change, Topic 3 of the Model Inter-Comparison Study for Asia Phase III (MICS-Asia III) –
850 Part 1: Overview and model evaluation, Atmos. Chem. Phys., 18, 4859-4884, 2018.
- 851 Geng, G., Zheng, Y., Zhang, Q., Xue, T., Zhao, H., Tong, D., Zheng, B., Li, M., Liu, F., Hong,
852 C., He, K., and Davis, S. J.: Drivers of PM_{2.5} air pollution deaths in China 2002–2017, Nature
853 Geoscience, 14, 645-650, 2021.
- 854 Georgoulias, A. K., van der A, R. J., Stammes, P., Boersma, K. F., and Eskes, H. J.: Trends and
855 trend reversal detection in 2 decades of tropospheric NO₂ satellite observations, Atmos. Chem.
856 Phys., 19, 6269-6294, 2019.
- 857 Hammer, M. S., van Donkelaar, A., Li, C., Lyapustin, A., Sayer, A. M., Hsu, N. C., Levy, R. C.,
858 Garay, M. J., Kalashnikova, O. V., Kahn, R. A., Brauer, M., Apte, J. S., Henze, D. K., Zhang, L.,
859 Zhang, Q., Ford, B., Pierce, J. R., and Martin, R. V.: Global Estimates and Long-Term Trends of
860 Fine Particulate Matter Concentrations (1998–2018), Environmental Science & Technology, 54,
861 7879-7890, 2020.
- 862 Hou, Y., Wang, L., Zhou, Y., Wang, S., Liu, W., and Zhu, J.: Analysis of the tropospheric
863 column nitrogen dioxide over China based on satellite observations during 2008–2017,
864 Atmospheric Pollution Research, 10, 651-655, 2019.
- 865 Huang, X., Li, M., Li, J., and Song, Y.: A high-resolution emission inventory of crop burning in
866 fields in China based on MODIS Thermal Anomalies/Fire products, Atmospheric Environment,
867 50, 9-15, 2012a.
- 868 Huang, X., Song, Y., Li, M., Li, J., Huo, Q., Cai, X., Zhu, T., Hu, M., and Zhang, H.: A high-
869 resolution ammonia emission inventory in China, Global Biogeochemical Cycles, 26, 2012b.
- 870 Itahashi, S., Ge, B., Sato, K., Fu, J. S., Wang, X., Yamaji, K., Nagashima, T., Li, J., Kajino, M.,
871 Liao, H., Zhang, M., Wang, Z., Li, M., Kurokawa, J., Carmichael, G. R., and Wang, Z.: MICS-
872 Asia III: overview of model intercomparison and evaluation of acid deposition over Asia, Atmos.
873 Chem. Phys., 20, 2667-2693, 2020.
- 874 Itahashi, S., Yumimoto, K., Kurokawa, J.-i., Morino, Y., Nagashima, T., Miyazaki, K., Maki, T.,
875 and Ohara, T.: Inverse estimation of NO_x emissions over China and India 2005–2016:
876 contrasting recent trends and future perspectives, Environmental Research Letters, 14, 124020,
877 2019.
- 878 Jacob, D. J. and Winner, D. A.: Effect of climate change on air quality, Atmospheric
879 Environment, 43, 51-63, 2009.



- 880 Janssens-Maenhout, G., Crippa, M., Guizzardi, D., Dentener, F., Muntean, M., Pouliot, G.,
881 Keating, T., Zhang, Q., Kurokawa, J., Wankmüller, R., Denier van der Gon, H., Kuenen, J. J. P.,
882 Klimont, Z., Frost, G., Darras, S., Koffi, B., and Li, M.: HTAP_v2.2: a mosaic of regional and
883 global emission grid maps for 2008 and 2010 to study hemispheric transport of air pollution,
884 *Atmos. Chem. Phys.*, 15, 11411-11432, 2015.
- 885 Janssens-Maenhout, G., Crippa, M., Guizzardi, D., Muntean, M., Schaaf, E., Dentener, F.,
886 Bergamaschi, P., Pagliari, V., Olivier, J. G. J., Peters, J. A. H. W., van Aardenne, J. A., Monni,
887 S., Doering, U., Petrescu, A. M. R., Solazzo, E., and Oreggioni, G. D.: EDGAR v4.3.2 Global
888 Atlas of the three major greenhouse gas emissions for the period 1970–2012, *Earth Syst. Sci.*
889 *Data*, 11, 959-1002, 2019.
- 890 Jiang, Z., Worden, J. R., Worden, H., Deeter, M., Jones, D. B. A., Arellano, A. F., and Henze, D.
891 K.: A 15-year record of CO emissions constrained by MOPITT CO observations, *Atmos. Chem.*
892 *Phys.*, 17, 4565-4583, 2017.
- 893 Kang, Y., Liu, M., Song, Y., Huang, X., Yao, H., Cai, X., Zhang, H., Kang, L., Liu, X., Yan, X.,
894 He, H., Zhang, Q., Shao, M., and Zhu, T.: High-resolution ammonia emissions inventories in
895 China from 1980 to 2012, *Atmos. Chem. Phys.*, 16, 2043-2058, 2016.
- 896 Kim, J., Jeong, U., Ahn, M.-H., Kim, J. H., Park, R. J., Lee, H., Song, C. H., Choi, Y.-S., Lee,
897 K.-H., Yoo, J.-M., Jeong, M.-J., Park, S. K., Lee, K.-M., Song, C.-K., Kim, S.-W., Kim, Y. J.,
898 Kim, S.-W., Kim, M., Go, S., Liu, X., Chance, K., Chan Miller, C., Al-Saadi, J., Veihelmann, B.,
899 Bhartia, P. K., Torres, O., Abad, G. G., Haffner, D. P., Ko, D. H., Lee, S. H., Woo, J.-H., Chong,
900 H., Park, S. S., Nicks, D., Choi, W. J., Moon, K.-J., Cho, A., Yoon, J., Kim, S.-k., Hong, H., Lee,
901 K., Lee, H., Lee, S., Choi, M., Veefkind, P., Levelt, P. F., Edwards, D. P., Kang, M., Eo, M.,
902 Bak, J., Baek, K., Kwon, H.-A., Yang, J., Park, J., Han, K. M., Kim, B.-R., Shin, H.-W., Choi,
903 H., Lee, E., Chong, J., Cha, Y., Koo, J.-H., Irie, H., Hayashida, S., Kasai, Y., Kanaya, Y., Liu,
904 C., Lin, J., Crawford, J. H., Carmichael, G. R., Newchurch, M. J., Lefer, B. L., Herman, J. R.,
905 Swap, R. J., Lau, A. K. H., Kurosu, T. P., Jaross, G., Ahlers, B., Dobber, M., McElroy, C. T.,
906 and Choi, Y.: New Era of Air Quality Monitoring from Space: Geostationary Environment
907 Monitoring Spectrometer (GEMS), *Bulletin of the American Meteorological Society*, 101, E1-
908 E22, 2020.
- 909 Klausbrückner, C., Annegarn, H., Henneman, L. R. F., and Rafaj, P.: A policy review of
910 synergies and trade-offs in South African climate change mitigation and air pollution control
911 strategies, *Environmental Science & Policy*, 57, 70-78, 2016.
- 912 Koukouli, M. E., Theys, N., Ding, J., Zyrichidou, I., Mijling, B., Balis, D., and van der A, R. J.:
913 Updated SO₂ emission estimates over China using OMI/Aura observations, *Atmos. Meas. Tech.*,
914 11, 1817-1832, 2018.
- 915 Krotkov, N. A., McLinden, C. A., Li, C., Lamsal, L. N., Celarier, E. A., Marchenko, S. V.,
916 Swartz, W. H., Bucsel, E. J., Joiner, J., Duncan, B. N., Boersma, K. F., Veefkind, J. P., Levelt,
917 P. F., Fioletov, V. E., Dickerson, R. R., He, H., Lu, Z., and Streets, D. G.: Aura OMI
918 observations of regional SO₂ and NO₂ pollution changes from 2005 to 2015, *Atmos. Chem.*
919 *Phys.*, 16, 4605-4629, 2016.



- 920 Kurokawa, J. and Ohara, T.: Long-term historical trends in air pollutant emissions in Asia:
921 Regional Emission inventory in ASia (REAS) version 3, *Atmos. Chem. Phys.*, 20, 12761-12793,
922 2020.
- 923 Lee, D.-G., Lee, Y.-M., Jang, K.-W., Yoo, C., Kang, K.-H., Lee, J.-H., Jung, S.-W., Park, J.-M.,
924 Lee, S.-B., Han, J.-S., Hong, J.-H., and Lee, S.-J.: Korean National Emissions Inventory System
925 and 2007 Air Pollutant Emissions, *Asian Journal of Atmospheric Environment*, 5, 278-291,
926 2011.
- 927 Li, C., McLinden, C., Fioletov, V., Krotkov, N., Carn, S., Joiner, J., Streets, D., He, H., Ren, X.,
928 Li, Z., and Dickerson, R. R.: India Is Overtaking China as the World's Largest Emitter of
929 Anthropogenic Sulfur Dioxide, *Scientific Reports*, 7, 14304, 2017a.
- 930 Li, K., Jacob, D. J., Liao, H., Zhu, J., Shah, V., Shen, L., Bates, K. H., Zhang, Q., and Zhai, S.: A
931 two-pollutant strategy for improving ozone and particulate air quality in China, *Nature*
932 *Geoscience*, 12, 906-910, 2019a.
- 933 Li, M., Klimont, Z., Zhang, Q., Martin, R. V., Zheng, B., Heyes, C., Cofala, J., Zhang, Y., and
934 He, K.: Comparison and evaluation of anthropogenic emissions of SO₂ and NO_x over China,
935 *Atmos. Chem. Phys.*, 18, 3433-3456, 2018.
- 936 Li, M., Liu, H., Geng, G., Hong, C., Liu, F., Song, Y., Tong, D., Zheng, B., Cui, H., Man, H.,
937 Zhang, Q., and He, K.: Anthropogenic emission inventories in China: a review, *National Science*
938 *Review*, 4, 834-866, 2017b.
- 939 Li, M., Zhang, Q., Kurokawa, J. I., Woo, J. H., He, K., Lu, Z., Ohara, T., Song, Y., Streets, D.
940 G., Carmichael, G. R., Cheng, Y., Hong, C., Huo, H., Jiang, X., Kang, S., Liu, F., Su, H., and
941 Zheng, B.: MIX: a mosaic Asian anthropogenic emission inventory under the international
942 collaboration framework of the MICS-Asia and HTAP, *Atmos. Chem. Phys.*, 17, 935-963,
943 2017c.
- 944 Li, M., Zhang, Q., Streets, D. G., He, K. B., Cheng, Y. F., Emmons, L. K., Huo, H., Kang, S. C.,
945 Lu, Z., Shao, M., Su, H., Yu, X., and Zhang, Y.: Mapping Asian anthropogenic emissions of
946 non-methane volatile organic compounds to multiple chemical mechanisms, *Atmos. Chem.*
947 *Phys.*, 14, 5617-5638, 2014.
- 948 Li, M., Zhang, Q., Zheng, B., Tong, D., Lei, Y., Liu, F., Hong, C., Kang, S., Yan, L., Zhang, Y.,
949 Bo, Y., Su, H., Cheng, Y., and He, K.: Persistent growth of anthropogenic non-methane volatile
950 organic compound (NMVOC) emissions in China during 1990–2017: drivers, speciation and
951 ozone formation potential, *Atmos. Chem. Phys.*, 19, 8897-8913, 2019b.
- 952 Liu, F., Zhang, Q., Tong, D., Zheng, B., Li, M., Huo, H., and He, K. B.: High-resolution
953 inventory of technologies, activities, and emissions of coal-fired power plants in China from
954 1990 to 2010, *Atmos. Chem. Phys.*, 15, 13299-13317, 2015.
- 955 Liu, F., Zhang, Q., van der A, R. J., Zheng, B., Tong, D., Yan, L., Zheng, Y., and He, K.: Recent
956 reduction in NO_x emissions over China: synthesis of satellite observations and emission
957 inventories, *Environmental Research Letters*, 11, 114002, 2016.



- 958 Lu, Z. and Streets, D. G.: Increase in NO_x Emissions from Indian Thermal Power Plants during
959 1996–2010: Unit-Based Inventories and Multisatellite Observations, *Environmental Science &*
960 *Technology*, 46, 7463-7470, 2012.
- 961 Lu, Z., Zhang, Q., and Streets, D. G.: Sulfur dioxide and primary carbonaceous aerosol
962 emissions in China and India, 1996–2010, *Atmos. Chem. Phys.*, 11, 9839-9864, 2011.
- 963 McDuffie, E. E., Smith, S. J., O'Rourke, P., Tibrewal, K., Venkataraman, C., Marais, E. A.,
964 Zheng, B., Crippa, M., Brauer, M., and Martin, R. V.: A global anthropogenic emission
965 inventory of atmospheric pollutants from sector- and fuel-specific sources (1970–2017): an
966 application of the Community Emissions Data System (CEDS), *Earth Syst. Sci. Data*, 12, 3413-
967 3442, 2020.
- 968 Miyazaki, K., Eskes, H., Sudo, K., Boersma, K. F., Bowman, K., and Kanaya, Y.: Decadal
969 changes in global surface NO_x emissions from multi-constituent satellite data assimilation,
970 *Atmos. Chem. Phys.*, 17, 807-837, 2017.
- 971 Mo, Z., Shao, M., and Lu, S.: Compilation of a source profile database for hydrocarbon and
972 OVOC emissions in China, *Atmospheric Environment*, 143, 209-217, 2016.
- 973 Phillips, D.: Ambient Air Quality Synergies with a 2050 Carbon Neutrality Pathway in South
974 Korea, *Climate*, 10, 1, 2022.
- 975 Qu, Z., Henze, D. K., Li, C., Theys, N., Wang, Y., Wang, J., Wang, W., Han, J., Shim, C.,
976 Dickerson, R. R., and Ren, X.: SO₂ Emission Estimates Using OMI SO₂ Retrievals for 2005–
977 2017, *Journal of Geophysical Research: Atmospheres*, 124, 8336-8359, 2019.
- 978 Saari, R. K., Selin, N. E., Rausch, S., and Thompson, T. M.: A self-consistent method to assess
979 air quality co-benefits from U.S. climate policies, *Journal of the Air & Waste Management*
980 *Association*, 65, 74-89, 2015.
- 981 Samset, B. H., Lund, M. T., Bollasina, M., Myhre, G., and Wilcox, L.: Emerging Asian aerosol
982 patterns, *Nature Geoscience*, 12, 582-584, 2019.
- 983 Shibata, Y. and Morikawa, T.: Review of the JCAP/JATOP Air Quality Model Study in Japan,
984 *Atmosphere*, 12, 943, 2021.
- 985 Simon, H., Beck, L., Bhave, P. V., Divita, F., Hsu, Y., Luecken, D., Mobley, J. D., Pouliot, G.
986 A., Reff, A., Sarwar, G., and Strum, M.: The development and uses of EPA's SPECIATE
987 database, *Atmospheric Pollution Research*, 1, 196-206, 2010.
- 988 Song, Y., Liu, B., Miao, W., Chang, D., and Zhang, Y.: Spatiotemporal variation in
989 nonagricultural open fire emissions in China from 2000 to 2007, *Global Biogeochemical Cycles*,
990 23, 2009.
- 991 Stavrou, T., Müller, J.-F., Bauwens, M., and De Smedt, I.: Sources and Long-Term Trends of
992 Ozone Precursors to Asian Pollution. In: *Air Pollution in Eastern Asia: An Integrated*
993 *Perspective*, Bouarar, I., Wang, X., and Brasseur, G. P. (Eds.), Springer International Publishing,
994 Cham, 2017.



- 995 Van Damme, M., Clarisse, L., Franco, B., Sutton, M. A., Erisman, J. W., Wichink Kruit, R., van
996 Zanten, M., Whitburn, S., Hadji-Lazaro, J., Hurtmans, D., Clerbaux, C., and Coheur, P.-F.:
997 Global, regional and national trends of atmospheric ammonia derived from a decadal (2008–
998 2018) satellite record, *Environmental Research Letters*, 16, 055017, 2021.
- 999 van der A, R. J., Mijling, B., Ding, J., Koukouli, M. E., Liu, F., Li, Q., Mao, H., and Theys, N.:
1000 Cleaning up the air: effectiveness of air quality policy for SO₂ and NO_x emissions in China,
1001 *Atmos. Chem. Phys.*, 17, 1775-1789, 2017.
- 1002 van der Werf, G. R., Randerson, J. T., Giglio, L., van Leeuwen, T. T., Chen, Y., Rogers, B. M.,
1003 Mu, M., van Marle, M. J. E., Morton, D. C., Collatz, G. J., Yokelson, R. J., and Kasibhatla, P. S.:
1004 Global fire emissions estimates during 1997–2016, *Earth Syst. Sci. Data*, 9, 697-720, 2017.
- 1005 von Schneidemesser, E. and Monks, P. S.: Air quality and climate – synergies and trade-offs,
1006 *Environmental Science: Processes & Impacts*, 15, 1315-1325, 2013.
- 1007 Woo, J.-H., Choi, K.-C., Kim, H. K., Baek, B. H., Jang, M., Eum, J.-H., Song, C. H., Ma, Y.-I.,
1008 Sunwoo, Y., Chang, L.-S., and Yoo, S. H.: Development of an anthropogenic emissions
1009 processing system for Asia using SMOKE, *Atmospheric Environment*, 58, 5-13, 2012.
- 1010 Xiao, Q., Li, M., Liu, H., Fu, M., Deng, F., Lv, Z., Man, H., Jin, X., Liu, S., and He, K.:
1011 Characteristics of marine shipping emissions at berth: profiles for particulate matter and volatile
1012 organic compounds, *Atmos. Chem. Phys.*, 18, 9527-9545, 2018.
- 1013 Yin, L., Du, P., Zhang, M., Liu, M., Xu, T., and Song, Y.: Estimation of emissions from biomass
1014 burning in China (2003–2017) based on MODIS fire radiative energy data, *Biogeosciences*, 16,
1015 1629-1640, 2019.
- 1016 Yuan, B., Shao, M., Lu, S., and Wang, B.: Source profiles of volatile organic compounds
1017 associated with solvent use in Beijing, China, *Atmospheric Environment*, 44, 1919-1926, 2010.
- 1018 Zhang, C., Liu, C., Hu, Q., Cai, Z., Su, W., Xia, C., Zhu, Y., Wang, S., and Liu, J.: Satellite UV-
1019 Vis spectroscopy: implications for air quality trends and their driving forces in China during
1020 2005–2017, *Light: Science & Applications*, 8, 100, 2019.
- 1021 Zhang, Y., Cooper, O. R., Gaudel, A., Thompson, A. M., Nédélec, P., Ogino, S.-Y., and West, J.
1022 J.: Tropospheric ozone change from 1980 to 2010 dominated by equatorward redistribution
1023 of emissions, *Nature Geoscience*, 9, 875-879, 2016.
- 1024 Zhang, Y., West, J. J., Emmons, L. K., Flemming, J., Jonson, J. E., Lund, M. T., Sekiya, T.,
1025 Sudo, K., Gaudel, A., Chang, K.-L., Nédélec, P., and Thouret, V.: Contributions of World
1026 Regions to the Global Tropospheric Ozone Burden Change From 1980 to 2010, *Geophysical
1027 Research Letters*, 48, e2020GL089184, 2021.
- 1028 Zheng, B., Cheng, J., Geng, G., Wang, X., Li, M., Shi, Q., Qi, J., Lei, Y., Zhang, Q., and He, K.:
1029 Mapping anthropogenic emissions in China at 1 km spatial resolution and its application in air
1030 quality modeling, *Science Bulletin*, 66, 612-620, 2021.
- 1031 Zheng, B., Chevallier, F., Yin, Y., Ciais, P., Fortems-Cheiney, A., Deeter, M. N., Parker, R. J.,
1032 Wang, Y., Worden, H. M., and Zhao, Y.: Global atmospheric carbon monoxide budget 2000–



- 1033 2017 inferred from multi-species atmospheric inversions, *Earth Syst. Sci. Data*, 11, 1411-1436,
1034 2019.
- 1035 Zheng, B., Huo, H., Zhang, Q., Yao, Z. L., Wang, X. T., Yang, X. F., Liu, H., and He, K. B.:
1036 High-resolution mapping of vehicle emissions in China in 2008, *Atmos. Chem. Phys.*, 14, 9787-
1037 9805, 2014.
- 1038 Zheng, B., Tong, D., Li, M., Liu, F., Hong, C., Geng, G., Li, H., Li, X., Peng, L., Qi, J., Yan, L.,
1039 Zhang, Y., Zhao, H., Zheng, Y., He, K., and Zhang, Q.: Trends in China's anthropogenic
1040 emissions since 2010 as the consequence of clean air actions, *Atmos. Chem. Phys.*, 18, 14095-
1041 14111, 2018.
- 1042